

MICROCOPY RESOLUTION TEST CHART  
NATIONAL BUREAU OF STANDARDS-1963 A

ADA 130423

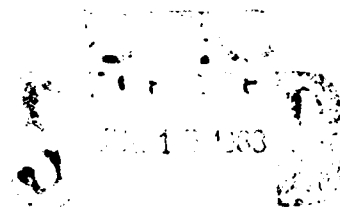
MAR. INCORPORATED  
131 BOSTON POST ROAD  
EAST LYME, CONNECTICUT 06333  
(203) 739-6996

**CHEMICAL SOUND ABSORPTION IN SEA WATER:  
LOW-FREQUENCY RELAXATION MECHANISM**

by  
**Dr. Robert H. Mellen**

**April 1983**

**Technical Report No. 335N  
Contract N00014-82-C-0161**



**Prepared for:  
Code S2101A**

**DEPARTMENT OF THE NAVY  
OFFICE OF NAVAL RESEARCH  
800 N. Quincy Street  
Arlington, VA 22217**

Approved For	
Dist	A

This document has been approved for public release and sale; its distribution is unlimited.

## TABLE OF CONTENTS

LIST OF ILLUSTRATIONS . . . . .	i
LIST OF TABLES. . . . .	iii
Section	Page
1 BACKGROUND. . . . .	1-1
2 ANALYSIS. . . . .	2-1
2.1 Sea Water Chemistry . . . . .	2-1
2.2 Relaxation Kinetics . . . . .	2-10
2.3 Resonator Method . . . . .	2-17
2.4 Boric Acid. . . . .	2-21
2.5 Synthetic Sea Water . . . . .	2-26
3 DISCUSSION. . . . .	3-1
4 CONCLUSIONS . . . . .	4-1
REFERENCES. . . . .	R-1

## LIST OF ILLUSTRATIONS

Figure	Page
1-1 Thorp's Compilation of Low-Frequency Attenuation Data Compared With the Marsh-Schulkin Formula (Second term in the equation for solid curve is the 1 kHz relaxation.) . . . . .	1-3
2-1 Lyman's Sea Water Dilution Data Compared With SSW Ionization Model for $B(OH)_3$ Showing the Relative Contributions of the Three Ion-Pairs . . . . .	2-6
2-2 Lyman's Sea Water Dilution Data Compared With SSW Model for the Second Ionization of $CO_2$ Showing the Relative Contributions of the Three Ion-Pairs. . . . .	2-7
2-3 Apparent Molal Volumes of Boric Acid and Sodium Borate in $H_2O$ Solution vs. Concentration. . . . .	2-9

## LIST OF ILLUSTRATIONS (Cont'd)

Figure		Page
2-4	Schematic of Resonator Apparatus. . . . .	2-18
2-5	Simmons' T-jump Measurements of Relaxation Frequency vs. Concentration in Synthetic Sea Water and in 0.725M NaCl Solution. . . . .	2-23
2-6	Resonator Measurements of $\alpha_{\max}$ vs. Concentration in Aqueous $B(OH)_3$ Compared to Theory. . . . .	2-27
2-7	Resonator Measurements of $\alpha_{\max}$ vs. pH in Aqueous $B(OH)_3$ Compared to Theory . . . . .	2-28
2-8	$B(OH)_3$ Absorption Spectra in Na/ $CO_2$ System as a Function of $NaHCO_3$ Concentration at pH = 9.0. . . . .	2-30
2-9	$B(OH)_3$ Absorption Spectra in Ca/ $CO_2$ System as a Function of $B(OH)_3$ Concentration at pH = 9.1. . . . .	2-32
2-10	Relaxation Frequency vs. Effective Concentration. . . . .	2-34
2-11	$\alpha_{\max}$ vs. Concentration Product Compared With Theory (Values of $\Delta V$ are calculated.) . . . . .	2-36
2-12	$\alpha_{\max}$ vs. pH in $B(OH)_3/CO_2/Ca$ System Compared With Aqueous Boric Acid and Borax Results of Figure 2-7 . . . . .	2-37
2-13	$B(OH)_3$ Absorption Spectrum in SSW With 4.6 X $B(OH)_3$ Concentration and NaCl Omitted Showing the Estimated Three Relaxation Components (Without Ca the $B(OH)_3$ component is estimated to be lower by roughly a factor of 10.) . . . . .	2-39
2-14	Absorption at 12 kHz vs. pH Estimated for the Three Components of Figure 2-13 (NaCl is omitted; values are $pK_B^*$ 8.92, $pK_{2C}^*$ 9.21.) . . . . .	2-40
2-15	Absorption vs. pH at 12 kHz Estimated for the Three Relaxation Components at 9°C (NaCl is included; values are $pK_B^*$ 8.85, $pK_{2C}^*$ 9.28.) . . . . .	2-41

## LIST OF ILLUSTRATIONS (Cont'd)

Figure		Page
2-16	Absorption vs. pH at 12 kHz Estimated for the Three Relaxation Components at 27°C (NaCl is included; values are $pK_B^*$ 8.90, $pK_{2C}^*$ 9.05.) . . . . .	2-42
2-17	$B(OH)_3$ ( $\alpha\lambda$ ) <sub>max</sub> vs. pH Relative to Thorp's Values at pH = 8.0 and 4°C Comparing Sea Data and Resonator Values . . . . .	2-44
3-1	Simmons' T-jump Measurements of $B(OH)_3$ Relaxation Frequency vs. Concentration in SSW Compared With Two-step and Exchange Theories . . . . .	3-2
3-2	T-jump Measurements of $B(OH)_3$ Relaxation Frequency vs. pH in Sea Water Compared With Two-step and Exchange Theories . . . . .	3-3
3-3	T-jump Measurements of $B(OH)_3$ Relaxation Frequency in NaCl Solution Compared With Present Theory . . . . .	3-5
3-4	T-jump Measurements of $B(OH)_3$ Relaxation Frequency in SSW Compared With Present Theory . . . . .	3-10

## LIST OF TABLES

Table		Page
2-1	Synthetic Sea Water Recipe (No Sulfate) . . . . .	2-3
2-2	$B(OH)_3$ Rate and Equilibrium Constants Calculated Using Apparent Constants $pK_w^* = 13.77$ and $pK_B^* = 8.83$ With Estimated Diffusion-Control Value for $k_1^+$ (Simmons Theory) . . . . .	2-25
3-1	$B(OH)_3$ Rate and Equilibrium Constants in NaCl Solution (Present Theory) . . . . .	3-6

## EXECUTIVE SUMMARY

Sound absorption is a major consideration in SONAR systems. Absorption in sea water involves pressure-dependent chemical equilibria with relatively slow relaxation rates. Understanding the mechanism is essential to account for effects of variable environmental factors.

Boric acid was identified as the cause of low-frequency absorption by means of a temperature-jump (T-jump) method which measures rate of change of pH. Concentration studies showed that the relaxation frequency never exceeds 4 kHz in either fresh water or synthetic sea water. Results in both cases are consistent with a rapid hydroxyl association followed by the rate-controlling monomolecular step. However, theoretical absorption predictions are much too low in either case.

Absorption measurements in synthetic sea water by the resonator method now show that the relaxation frequency can not only exceed 4 kHz, but also depends on the concentration of carbonic acid as well as boric acid. In addition, absorption depends on the concentration product. These results are consistent with a slow single-step exchange reaction which does not involve change in pH. Coupling to the fast  $\text{CaCO}_3$  ion-pair equilibrium is also important because absorption is too small if calcium is omitted.

The discrepancy between resonator and T-jump measurements is resolved if both steps of the hydroxyl association are slow. In sea water, the coupled system then has two slow relaxations, the association controlling pH and the exchange controlling absorption.

It is concluded that the dominant low-frequency absorption mechanism in sea water is the exchange reaction and that the laboratory measurements of synthetic sea water are completely consistent with the empirical formula derived from sea measurements.

## ADMINISTRATIVE INFORMATION

The scientific investigation and the development and preparation of this resulting Technical Report were performed for the Office of Naval Research under Navy Contract N00014-82-C-0161. The Scientific Officer and Technical Sponsor for this work is Dr. R. L. Sternberg, ONR Code 420.

The author of this report, Dr. R. H. Mellen, is a consultant to MAR, Incorporated's New England Division, East Lyme, CT.

## ABSTRACT

Low-frequency sound absorption in sea water is dominated by a 1 kHz relaxation involving boric acid. Resonator measurements in synthetic sea water show that the relaxation mechanism can be modeled as an exchange between the borate and carbonate equilibria in which coupling with calcium ion-pair equilibria provides most of the volume change. Consistency with the empirical pH-dependent absorption formula derived from ocean measurements is also demonstrated.

## Section 1

## BACKGROUND

The 1935 Naval Research Laboratory (NRL) report by Stephenson<sup>1</sup> appears to be the first to recognize that sound absorption in the ocean is much greater than in fresh water. However, it was not until after World War II, when the anomaly had been verified by extensive sea measurements, that efforts were undertaken to determine the cause. Laboratory measurements showed that fresh water absorption follows the classical frequency-squared dependence. The magnitude was found to be somewhat greater than predicted from shear viscosity, but this was eventually explained by bulk viscosity. The sea-water anomaly was more than an order of magnitude greater.

In 1948, Liebermann<sup>2</sup> reported field measurements comparing fresh water and sea water absorption in the common frequency range of 10 - 1000 kHz. Earlier sea data were concentrated in the SONAR range below 100 kHz, while fresh water had been measured at much higher frequencies. Measurements in a reservoir showed agreement with the earlier fresh water results. Sea measurements, on the other hand, agreed with earlier salt water values in the lower range, but decayed to fresh water values at high frequencies. A relaxation process was indicated.

Relaxational absorption can occur in chemical solutions as the result of pressure-dependent equilibria that affect the complex compressibility of the medium. The rate of equilibration determines the relaxation frequency which, in this case, was found to be 150 kHz. Liebermann proposed the ionization equilibrium of NaCl as a possible cause.

In 1949 Leonard, et al<sup>3</sup> reported initial results of a laboratory investigation of synthetic sea water (SSW) by the resonator method. The resonator a 12 liter spherical flask, was excited by acoustic pulses at selected resonant frequencies in the range of 25 - 500 kHz. The sphere was suspended in a vacuum chamber in order to minimize residual losses and improve sensitivity. Relaxational absorption spectra derived from measurements of decay rate showed  $MgSO_4$  to be the cause of the 150 kHz relaxation. A more detailed paper by Wilson and Leonard<sup>4</sup> appeared in 1954.

In 1953, Kurtze and Tamm<sup>5</sup> also confirmed Leonard's findings and, in addition, investigated the interactive effects of NaCl. A number of possible mechanisms were proposed. However, it was not until 1962, in a definitive analysis of Eigen and Tamm,<sup>6</sup> that the details of the multi-step  $MgSO_4$  mechanism were delineated.

In 1962, Schulkin and Marsh<sup>7</sup> introduced a formula for sound absorption in sea water based on the  $MgSO_4$  results and ocean measurements in the frequency range of 2 - 25 kHz. When the focus of attention in underwater acoustics shifted to lower frequencies, the validity of extrapolating the formula was subject to question.

In 1965, Thorp,<sup>8</sup> in a summary of low-frequency attenuation measurements, found values consistently an order of magnitude greater than predicted (figure 1-1). He also showed that the excess could be modeled as a 1 kHz relaxation.<sup>9</sup> Similar measurements in the Mediterranean by Skretting and Leroy showed a 1.7 kHz relaxation.<sup>10</sup> A chemical relaxation similar to  $MgSO_4$  seemed to be the most promising explanation.

To investigate the proposed second chemical relaxation, Browning, et al<sup>11</sup> carried out a series of sound channel propagation measurements with different ambient temperatures. A systematic increase in relaxation frequency

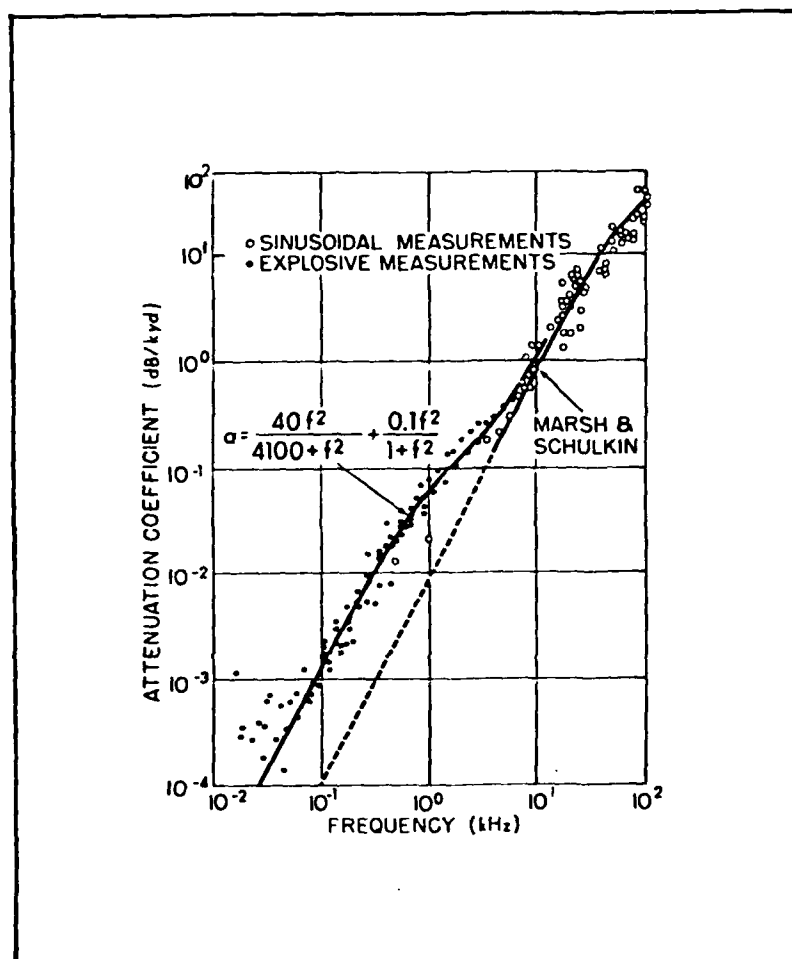


Figure 1-1. Thorp's Compilation of Low-Frequency Attenuation Data Compared With the Marsh-Schulkin Formula (Second term in the equation for solid curve is the 1 kHz relaxation.)

with temperature would be expected. Fresh water experiments were included for comparison purposes. Reports and publications resulting from this program are compiled in reference 12.

Results from Lake Superior<sup>13</sup> showed low-frequency attenuation comparable to Thorp's anomaly suggesting that sea salts might not be responsible. However, the Lake Tanganyika experiment<sup>14</sup> gave no evidence of a low-frequency relaxation and the hypothesis was abandoned. The Lake Superior anomaly was subsequently ascribed to leakage caused by scattering from random inhomogeneities in the thermocline. Frequency-independent attenuation, as the result of diffusion, is apparently common to all sound-channel experiments. However, the loss is usually small and detectable only at very low frequencies because of masking by absorption.<sup>15</sup>

Lake Tanganyika results also showed excess high-frequency loss similar to the  $\text{MgSO}_4$  relaxation in sea water. This lake is unusually high in carbonate, but magnesium and sulfate concentrations are much too low for  $\text{MgSO}_4$  to be responsible. Investigation of synthetic lake water by the resonator method showed the cause to be a similar  $\text{MgCO}_3$  relaxation.<sup>16</sup> The same relaxation also occurs in sea water, but it is only a minor absorption component compared to the others.<sup>17</sup>

Results of a number of sea experiments were then fitted by a Thorp-type equation plus a frequency-independent loss term.<sup>15</sup> Good correlation was found between relaxation frequency and temperature, indicating that a chemical relaxation was the likely mechanism. Considerable spread in the absorption coefficients was also noted. Following the discovery of boric acid as the cause of the relaxation, correlation with pH also showed the predicted behavior.<sup>18</sup>

Because of size limitations, the resonator method is not practical for investigating a relaxation in the 1 kHz range. In 1973, Yeager, et al<sup>19</sup>

employed the T-jump method to study the mechanism. The relaxation frequency was determined from the rate of change of pH following a sudden increase in temperature. Synthetic sea water measurements showed a relaxation in the 1 kHz range only with boric acid present. An acid-base exchange between the borate and carbonate equilibria was proposed as the likely mechanism, and possible interactive effects of ion-pairing were also pointed out.

In 1975, Simmons<sup>20</sup> reported a T-jump study of relaxation frequency as a function of  $B(OH)_3$  concentration. Results for synthetic sea water and NaCl solution were both fitted by two-step processes. Absorption measurements were also made in the frequency range of 6 - 150 kHz using a 100 liter resonator. Combined results appeared to support the conclusion that the mechanisms are similar in both  $H_2O$  and sea water.

Since 1979, an investigation of sound absorption in sea water by the resonator method has been carried on by Mellen, et al.<sup>21-23</sup> Relaxations involving  $MgCO_3^0$  and  $MgB(OH)^+$  have been identified and modeled as two-step processes incorporating interactive effects. However, attempts to model the  $B(OH)_3$  relaxation by a similar process proved unsuccessful.

In this report, analysis of the resonator measurements is presented which supports the first hypothesis, i.e., that the dominant process in sea water is an exchange between the borate and the carbonate equilibria in which calcium ion-pairing provides most of the volume change. In addition, consistency with the empirical pH-dependent absorption formula derived earlier from ocean measurements is demonstrated.

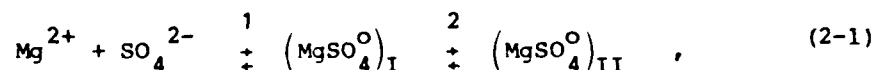
## Section 2

## ANALYSIS

## 2.1 SEA WATER CHEMISTRY

The simplifying assumption is that the concentrations of major sea water components vary only with salinity and remain in constant ratio. Concentrations of chemical species can depend additionally on temperature, pressure and pH. If the relaxation mechanisms are known in detail and specie concentrations and other parameters can be calculated, sound absorption should be predictable for any ocean conditions.

Specie concentrations depend on the properties of the various equilibria involved. In Leonard's experiments, the synthetic sea water constituents were  $\text{Na}_2\text{SO}_4$  and  $\text{MgCl}_2$ , while the relaxing species turned out to be  $\text{MgSO}_4$ . The multi-step relaxation can be represented for present purposes as the two-step equilibrium:



where step 2 controls the relaxation rate in question.

The stoichiometric association constant is

$$K_{\text{MgS}} = \frac{[\text{MgSO}_4^0]}{[\text{Mg}^{2+}][\text{SO}_4^{2-}]} = 10/M \quad (2-2)$$

where  $[\text{MgSO}_4^0] = [(\text{MgSO}_4^0)_I] + [(\text{MgSO}_4^0)_{II}]$ . Brackets indicate concentrations. Units of M are gram moles/liter. Values are for 25°C and atmospheric pressure.<sup>24</sup>

Common ions cause coupling between equilibria. In this example, the most important interaction is the fast reaction:



for which the association constant is

$$K_{\text{NaS}} = \frac{[\text{NaSO}_4^-]}{[\text{Na}^+][\text{SO}_4^{2-}]} = 2/M \quad (2-4)$$

Equilibrium "constants" may vary with ionic strength (Debye-Hückle effect). In conventional sea water stoichiometry, ionic strength is kept constant ( $I \sim 0.7$  M) while the ratios of the various components are varied. This is unnecessarily restrictive and very inefficient for absorption measurements because everything must be changed for each experiment. It is much more convenient simply to increase the concentration of the component under study, letting  $I$  change. Deviations from theory at low ionic strengths may result from variations in activity.

Not all major components of sea water affect  $\text{B}(\text{OH})_3$  absorption. Sulfate will be omitted throughout because the added  $\text{MgSO}_4$  absorption is an unnecessary complication. The essential constituents and concentrations for a synthetic sea water that satisfies the requirements of the present investigation are listed in table 2-1. Acid-base equilibria involving  $\text{B}(\text{OH})_3$  and  $\text{NaHCO}_3$  will be of concern. The  $\text{B}(\text{OH})_3/\text{B}(\text{OH})_4^-$  equilibrium shows no significant effects of variable activity. On the other hand,  $\text{HCO}_3^-/\text{CO}_3^{2-}$  activity changes, but becomes stabilized for  $I > 0.1$  M.

Table 2-1. Synthetic Sea Water Recipe  
(No Sulfate)

Constituent	Concentration (mM)
NaCl	400
MgCl <sub>2</sub>	50
CaCl <sub>2</sub>	10
NaHCO <sub>3</sub>	2.5
B(OH) <sub>3</sub>	0.43

The equilibrium constants of acid-base systems can be measured by pH variation as a function of concentration of the major pair-forming metallic ions; namely, Na<sup>+</sup>, Mg<sup>2+</sup>, and Ca<sup>2+</sup>. For example, in aqueous boric acid, the only significant species at concentrations less than 0.1 M are B(OH)<sub>3</sub> and B(OH)<sub>4</sub><sup>-</sup>. The equilibrium constant can be written

$$K_B = \frac{[B(OH)_4^-][H^+]}{[B(OH)_3]} = 5.9 \times 10^{-10} \text{ M} \quad (2-5)$$

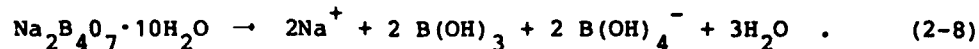
where [H<sup>+</sup>] is the hydrogen ion concentration. Only the borate ion forms pairs. Therefore, the apparent equilibrium constant in sea water can be written

$$K_B^* = \frac{[H^+] \left( [B(OH)_4^-] + [NaB(OH)_4^0] + [MgB(OH)_4^+] + [CaB(OH)_4^+] \right)}{[B(OH)_3]} \quad (2-6)$$

In terms of the association constants, equation (2-6) becomes

$$K_B^* = K_B \left( 1 + K_{NaB} [Na^+] + K_{MgB} [Mg^{2+}] + K_{CaB} [Ca^{2+}] \right) \quad (2-7)$$

The most straightforward method of measuring values is to use borax at low concentrations, e.g.,  $[B] \sim 10^{-3}$  M. At low concentration,  $Na^+$  ion-pairing is negligible and borax dissociation in  $H_2O$  yields



With  $[B(OH)_3] = [B(OH)_4^-]$  in Equation (2-5), we have  $K_B = [H^+]$  or  $pH = -\log [H^+] = pK_B = 9.23$ . When  $NaCl$ ,  $MgCl_2$  or  $CaCl_2$  are added,  $pH$  decreases because of ion-pairing and  $[H^+]$  increases to compensate for the reduced  $B(OH)_4^-$  concentration,  $K_B$  being constant. In equation (2-7), we then have  $K_B^* = [H^+]$  or  $pH = pK_B^* < 9.23$ . The charge conservation condition for changes in  $[H^+]$  can be neglected in the  $pH$  range of interest.

The ion-pair association constants can be determined by stepwise increasing the concentrations up to the sea water values. The respective equilibrium constants are calculated from the slope of  $K_B^*$  vs. concentration. The ion concentration can usually be approximated as the total concentration of the constituent, e.g.,  $[Na^+] \approx [NaCl]$ .

For calculating the boric acid concentration,

$$[B(OH)_3] = \frac{[B]}{1+x} \quad (2-9)$$

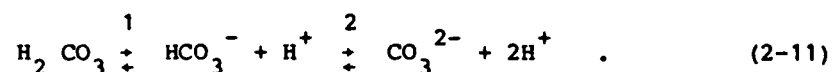
where  $x = 10^{pH - pK_B^*}$ . For the borate ion concentration,

$$[B(OH)_4^-] = \frac{[B] x}{1+x} \frac{1}{1 + K_{NaB} [Na^+] + K_{MgB} [Mg^{2+}] + K_{CaB} [Ca^{2+}]} \quad (2-10)$$

Other borate specie concentrations are obtained by multiplying the last term by the appropriate factor from the denominator.

The following values are indicated for sea water at 25°C:<sup>24</sup>  
 $K_{NaB} = 2.1/M$ ,  $K_{MgB} = 18/M$  and  $K_{CaB} = 26/M$ . In figure 2-1, the boric acid SSW model is compared to dilution measurements in CO<sub>2</sub>-free sea water by Lyman.<sup>25</sup> Agreement appears to support the overall validity of the SSW model.

In the CO<sub>2</sub> system, there are two equilibria to consider



The corresponding values are  $pK_{1C} \sim 6$  and  $pK_{2C} \sim 10$ . Only the second equilibrium appears to play any significant role in sea water absorption. Therefore, the first equilibrium can be neglected for  $pH > 7$ . The apparent equilibrium constant becomes

$$K_{2C}^* = K_{2C} \left( 1 + K_{Na2C} [Na^+] + K_{Mg2C} [Mg^{2+}] + K_{Ca2C} [Ca^{2+}] \right) \quad (2-12)$$

The following values are indicated for sea water at 25°C:<sup>24</sup>  $K_{Na2C} = 1.6/M$ ,  $K_{Mg2C} = 53/M$  and  $K_{Ca2C} = 125/M$ . In figure 2-2, the carbonate model is compared with Lyman's sea water dilution measurements of  $K_{2C}^*$ . Note that the nonlinear region near zero (dashed curve) may come from variations in the association constants as well as the  $K_{2C}$ . The stable value of  $K_{2C}$ , (horizontal dashed line) is  $1.8 \times 10^{-10}$  or  $pK_{2C} = 9.73$ , while the actual value is  $4.7 \times 10^{-11}$ , or  $pK_{2C}^0 = 10.33$ . Note that the slopes refer to the latter and are greater than the respective association constants by a factor of 4. The stable values are used for calculation of specie concentrations as in equations (2-9) and (2-10).

In addition to specie concentrations, values of the volume changes associated with the various equilibria are needed. Conventional units for  $\Delta V$  are milliliters/gram mole or liters/kilogram mole and will be abbreviated as /km.

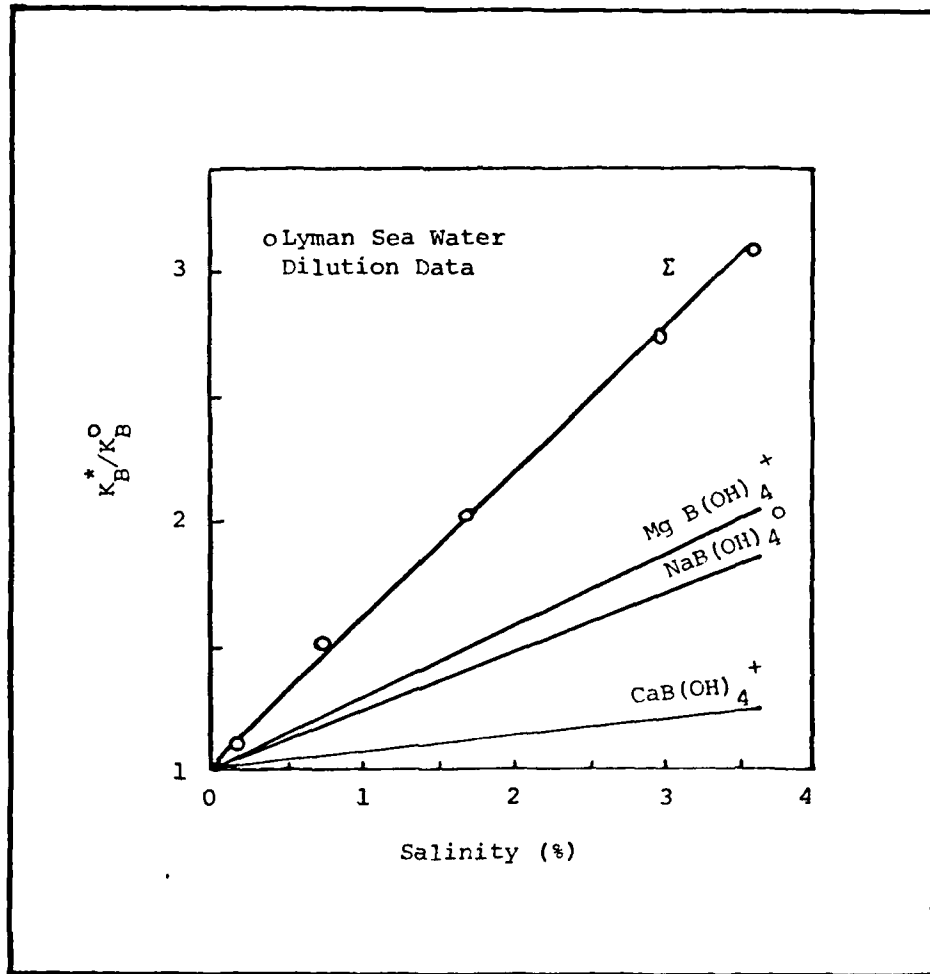


Figure 2-1. Lyman's Sea Water Dilution Data Compared With SSW Ionization Model for  $B(OH)_3$  Showing the Relative Contributions of the Three Ion-Pairs

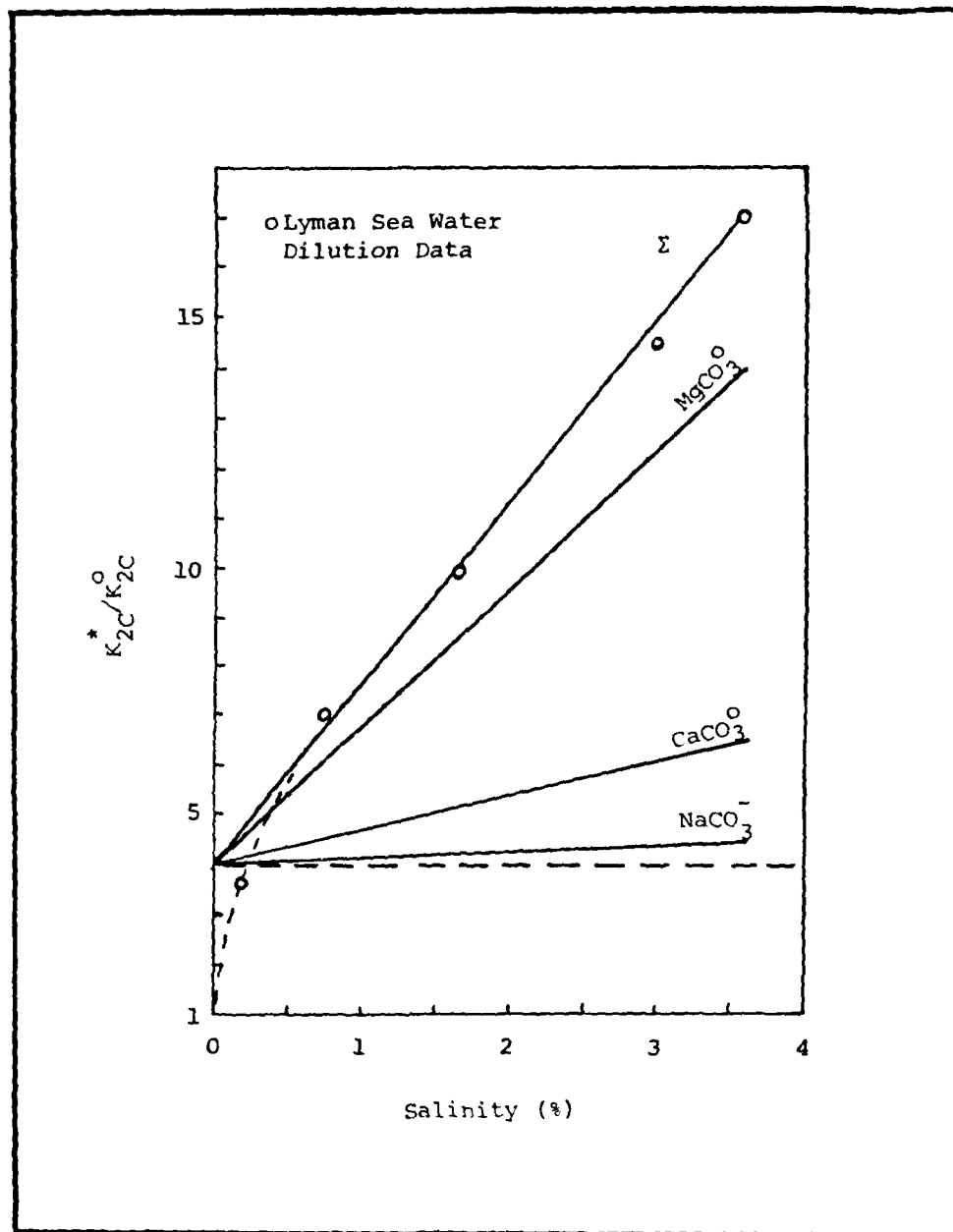


Figure 2-2. Lyman's Sea Water Dilution Data Compared With SSW Model for the Second Ionization of  $CO_2$  Showing the Relative Contributions of the Three Ion-Pairs

Apparent values may be calculated from measurements of the change of apparent equilibrium constants with pressure using the relation

$$\Delta V^* = \frac{-\partial \ln K^*}{\partial P} RT, \quad (2-13)$$

where T is absolute temperature and R is the gas constant.

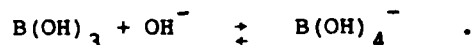
Another method is by measuring the density of solutions by means of the picnometer. Ward and Millero<sup>26</sup> used this method to study boric acid ionization in H<sub>2</sub>O. Measurements of B(OH)<sub>3</sub> and NaB(OH)<sub>4</sub> solution at 25°C are shown in figure 2-3. Constituent in the latter is sodium metaborate, which is assumed to dissociate as follows: NaBO<sub>2</sub>·2H<sub>2</sub>O + NaB(OH)<sub>4</sub><sup>0</sup> ⇌ Na<sup>+</sup> + B(OH)<sub>4</sub><sup>-</sup>. Note that the apparent molal volume of B(OH)<sub>3</sub> solution is 39.2/kM independent of concentration while ion-pairing in NaB(OH)<sub>4</sub> solution causes a progressive increase. At small concentration, association of NaB(OH)<sub>4</sub><sup>0</sup> is negligible and the apparent molal volume approaches

$$v^* \left( \text{NaB(OH)}_4 \right) = v^0 \left( \text{B(OH)}_4^- \right) + v^0 \left( \text{Na}^+ \right). \quad (2-14)$$

For  $v^0(\text{Na}^+) = -5.7/\text{kM}$ ,  $v^0 \left( \text{B(OH)}_4^- \right) = 20.7 + 5.7 = 26.4/\text{kM}$ . The value of  $\Delta V$  for boric acid ionization depends on which equilibrium is involved,



or



(2-15)

The volume change for formation of the ion-pair NaB(OH)<sub>4</sub><sup>0</sup> is calculated from curve fit to the data. For  $K_{\text{NaB}} = 2.1/\text{M}$ , the estimated value is  $\Delta V_{\text{NaB}} = 8/\text{kM}$ . Other values estimated from MgB(OH)<sub>4</sub><sup>+</sup> absorption measurements are  $\Delta V_{\text{MgB}} = 12/\text{kM}$ , and  $\Delta V_{\text{CaB}} = 0/\text{kM}$ .

Corresponding values for the CO<sub>2</sub> system are<sup>24</sup>  $\Delta V_{\text{Mg}2\text{C}} = 13.8/\text{kM}$ ,  $\Delta V_{\text{Na}2\text{C}} = 12/\text{kM}$ , and  $\Delta V_{\text{Ca}2\text{C}} = 12.5/\text{kM}$ .

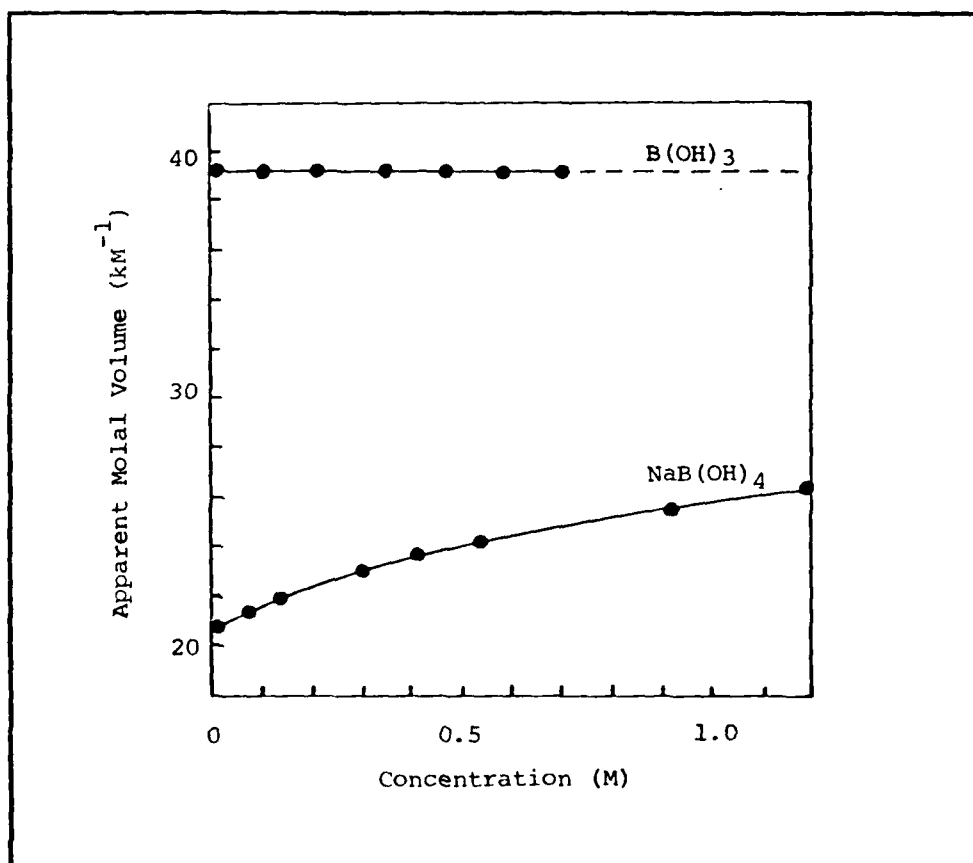


Figure 2-3. Apparent Molal Volumes of Boric Acid and Sodium Borate in H<sub>2</sub>O Solution vs. Concentration

## 2.2 RELAXATION KINETICS

The simplest case, representing a change in structure, is the monomolecular equilibrium<sup>27</sup>



The rate equation is

$$\frac{dA'}{dt} + k^+ A' - k^- B' = 0 \quad . \quad (2-17)$$

where  $k^+$  and  $k^-$  are forward and backward rate constants, respectively, and primes indicate instantaneous concentrations. For small perturbations, let

$$\begin{aligned} A' &= A + \Delta A \\ B' &= B + \Delta B \end{aligned} \quad , \quad (2-18)$$

where  $A$  and  $B$  are mean concentrations. Then  $\Delta A = -\Delta B$ .

Substituting equation (2-18) in equation (2-17) and using the equilibrium constant,

$$K = \frac{k^+}{k^-} = \frac{B}{A} \quad , \quad (2-19)$$

gives

$$\frac{d\Delta A}{dt} + (k^+ + k^-)\Delta A = 0 \quad . \quad (2-20)$$

A solution of equation (2-20) is

$$\Delta A = \Delta A_0 \exp(-t/\tau) \quad , \quad (2-21)$$

where  $\tau$  is the relaxation time. Then  $1/\tau = k^+ + k^- = \omega_r$  where  $\omega_r$  is the angular relaxation frequency.

For a sinusoidal forcing function equation (2-20) becomes

$$\tau \frac{d\Delta A}{dt} + \Delta A = Q \exp(i\omega t) , \quad (2-22)$$

where  $\omega$  is the angular frequency and  $Q$  is the amplitude. In this case the solution can be written

$$\Delta A = Q \exp(+i\omega t)/(1+i\omega\tau) . \quad (2-23)$$

An acoustic plane wave with attenuation can be written

$$Q = Q_0 \exp(-i\omega x/\bar{c}) = Q_0 \exp(-(\alpha+i\kappa)x) , \quad (2-24)$$

where  $\bar{c}$  is the complex sound speed. Taking the compressibility as the sum of the normal compressibility  $\beta_0 = (\rho_0 c_0^2)^{-1}$  and the relaxational compressibility  $\beta_r$ , the complex sound speed becomes

$$\bar{c} = \left( \rho_0 \left( \beta_0 + \beta_r / (1+i\omega\tau) \right) \right)^{-1/2} , \quad (2-25)$$

where  $\rho_0$  is density. Expanding the square root for small values and separating into real and imaginary parts, we find

$$\kappa = \frac{\omega}{c_0} \left( 1 + \frac{\beta_r}{2\beta_0} \frac{1}{1 + \omega^2\tau^2} \right) \quad (2-26)$$

$$\alpha = \frac{\omega}{c_0} \left( \frac{\beta_r}{2\beta_0} \frac{\omega\tau}{1 + \omega^2\tau^2} \right) .$$

The dispersion term is small and will be neglected. In some work, the attenuation coefficient in dimensionless form as  $\alpha\lambda$ , where  $\lambda$  is the acoustic wavelength. The absorption spectrum is then written as

$$\alpha\lambda = (\alpha\lambda)_{\max} \frac{2\omega\tau}{1 + \omega^2\tau^2} . \quad (2-27)$$

This approach may be useful for comparing measurements at different temperatures. However, in all but simple cases, it leads to extremely cumbersome equations. In this work, the alternative dimensional expression

$$\alpha = \alpha_{\max} \frac{\omega^2 \tau^2}{1 + \omega^2 \tau^2} \quad (2-28)$$

is used because the equations are much simpler and easier to understand. This fact can easily be verified by converting equations in  $\alpha_{\max}$  to  $(\alpha\lambda)_{\max}$  for the coupled reactions discussed later.

The chemical compressibility can be expressed in terms of other thermodynamic parameters. Simplifying approximations include neglect of enthalpy effects which are small when water is the solvent. For the case of equation (2-16), also neglecting activity effects, the chemical compressibility is

$$\beta_r = \frac{(\Delta V)^2}{RT} \left( \frac{1}{A} + \frac{1}{B} \right)^{-1}, \quad (2-29)$$

where  $\Delta V$  is the change in molal volume, i.e.,  $V_B - V_A$ .

Finally, substituting equation (2-29) in equation (2-26) and setting  $\beta_0 = (\rho_0 c_0^2)^{-1}$ ,

$$\alpha_{\max} = \frac{(\Delta V)^2 k^+ A \rho_0 c_0}{2 RT} \quad \text{Np/unit distance} . \quad (2-30)$$

Note that equation (2-30) can be written in a number of ways using the relations

$$k^+ A = k^- B = \frac{k^+ k^-}{k^+ + k^-} (A+B) . \quad (2-31)$$

Another simple case is the single-step association/dissociation equilibrium



By similar arguments,

$$\begin{aligned} \omega_r &= k^- + k^+ (A+B) \\ \alpha_{\max} &= \frac{(\Delta V)^2 k^+ AB \rho_{OC} c_0}{2RT} \quad , \end{aligned} \quad (2-33)$$

which can also be written other ways using the equilibrium condition  $K = k^+/k^- = C/AB$ . The two-step association proposed for aqueous  $B(OH)_3$  combines the two cases



The rate equations for this system are:

$$\text{and} \quad \frac{d\Delta A}{dt} + (k_1^- + k_1^+ (A+B)) \Delta A + k_1^- \Delta D = 0 \quad (2-35)$$

$$\frac{d\Delta D}{dt} + (k_2^- + k_2^+) \Delta D + k_2^+ \Delta A = 0 \quad .$$

When step 1 is diffusion-controlled, the upper relaxation frequency is given by equation (2-33). The parameters for the lower relaxation become

$$\text{and} \quad \omega_r = k_2^- + \frac{k_2^+ K_1 (A+B)}{1 + K_1 (A+B)} \quad (2-36)$$

$$\Delta V = \Delta V_2 + \frac{\Delta V_1}{1 + K_1 (A+B)} \quad .$$



When steps 2 and 3 are both slow, and steps 1, 4, and 5 are fast, there is only one slow relaxation. The relaxation frequency is given by

$$\omega_r = \frac{k_2^- + k_3^- K_5(D+E)}{1 + K_5(D+E)} + \frac{K_1(A+B) (k_2^+ + k_3^+ K_4(D+E))}{1 + K_1(A+B) (1 + K_4(D+E))} \quad (2-40)$$

The exchange or transfer equilibrium will be written<sup>28</sup>



In this case, the parameters are

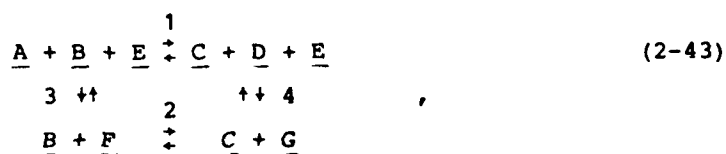
$$\omega_r = k^+(A+B) + k^-(C+D)$$

and

$$\alpha_{\max} = \frac{(\Delta V) k^+ AB \rho_o C_o}{2RT} \quad (2-42)$$

The equilibrium constant is given by  $K = k^+/k^- = CD/AB$ . For acid-base systems, we can also have the individual ionization constants; e.g.,  $K_1 = C[H^+]/A$  and  $K_2 = B[H^+]/D$ ; then  $K = K_1/K_2$ .

The coupled equilibria arising from ion-pairing will be written



where steps 3 and 4 are both fast. The association constants are  $K_3 = F/AE$  and  $K_4 = G/DE$ . For this system, we have only one slow relaxation and the parameters are

$$\omega_r = k_1^+ A + k_1^- D + k_2^+ (F+B) + k_2^- (C+G)$$

$$+ \frac{(k_1^- - k_2^-)C(1+K_3(A+E)+K_4D) + (k_1^+ - k_2^+)B(1+K_4(D+E)+K_3A)}{1 + K_3(A+E) + K_4(D+E) + K_3K_4E(A+D+E)},$$

$$\alpha_{\max} = \frac{(\Delta V)^2 (k_1^+ AB + k_2^+ FB) \rho_0 C_0}{2RT}, \quad (2-44)$$

and

$$\Delta V = \Delta V_1 - \frac{\Delta V_3 K_3 E (1+K_4(A+D+E)) - \Delta V_4 K_4 E (1+K_3(A+D+E))}{1 + K_3(A+E) + K_4(D+E) + K_3K_4E(A+D+E)}.$$

Finally, consider the coupling between the two-step and exchange reactions. The system will be

$$\frac{\underline{A} + \underline{B} + \underline{E}}{1} \rightleftharpoons \frac{\underline{C} + \underline{D} + \underline{E}}{2} \rightleftharpoons \frac{\underline{F} + \underline{B}}{4} \rightleftharpoons \frac{\underline{C} + \underline{B}}{4} \quad (2-45)$$

The rate equations for this system can be written

$$\frac{d\Delta A}{dt} + (k_3^+ B + k_1^- + k_1^+ (A+E)) \Delta A + (k_1^- - k_3^- D) \Delta C + (k_1^+ A - k_3^+ A - k_3^- C) \Delta D = 0,$$

$$\frac{d\Delta C}{dt} + (k_2^+ + k_3^+ B) \Delta A + (k_2^- + k_2^+ + k_3^- D) \Delta C + (k_3^+ A + k_3^- C) \Delta D = 0, \quad (2-46)$$

and

$$\frac{d\Delta D}{dt} + (k_4^+ D - k_3^+ B) \Delta A - k_3^- D \Delta C + (k_4^- + k_4^+ (D+E) + k_3^- C + k_3^+ A) \Delta D = 0.$$

If both steps 1 and 4 are diffusion-controlled, there is only one slow relaxation and the parameters are given by

$$\omega_r = k_2^- + k_3^- D - \frac{k_2^+ (K_1(A+E) + K_1K_4E(A+D+E)) + k_3^+ (K_4DA + B(1+K_4(D+E))) + k_3^- CK_4D}{1 + K_1(A+E) + K_4(D+E) + K_1K_4E(A+D+E)}$$

and (2-47)

$$\Delta V = \Delta V_3 - \frac{\Delta V_1 (K_1(A+E) + K_1K_4E(A+D+E)) - \Delta V_4 (1 + K_1(A+E) + K_4E + K_1K_4E(A+D+E))}{1 + K_1(A+E) + K_4(D+E) + K_1K_4E(A+D+E)}$$

In comparing calculations and measurements, frequency (f) will be expressed in Hz, where  $f = \omega/2\pi$ . Absorption units will be converted from Np to dB by multiplying by 8.7.

### 2.3 RESONATOR METHOD

The resonator apparatus is illustrated schematically in figure 2-4. The resonator used in these experiments is a 72-liter spherical boiling flask similar to the others. To minimize residual losses, it is suspended in a vacuum chamber by loops of piano wire as in the previous experiments.

The flask is also modified with a small ball-joint vacuum socket replacing the standard neck. The mating ball-joint is fitted with a pair of glass tubes which allow circulation of the liquid. Extending the input tube a few centimeters into the flask produces very efficient mixing by jet action. The exit tube is flush with the top inside surface so that air is not trapped. Flexible tubing is used to connect the glass tubes to a corresponding pair of metal tubes which pass through the cover plate of the vacuum chamber. Additional flexible tubing is also used to connect the external pump and reservoir to the system. In addition to storage of excess liquid, the reservoir serves for adding chemicals which are then circulated. In this way, the surrounding vacuum is not sacrificed and the resonator remains physically undisturbed.

The acidity of the solution is continuously monitored by means of a pH meter. Adjustment to a desired value is accomplished by adding concentrated hydrochloric acid or sodium hydroxide. Timing tests show that complete mixing is achieved in only 3 min. with the pump operating at 2 liters/min.

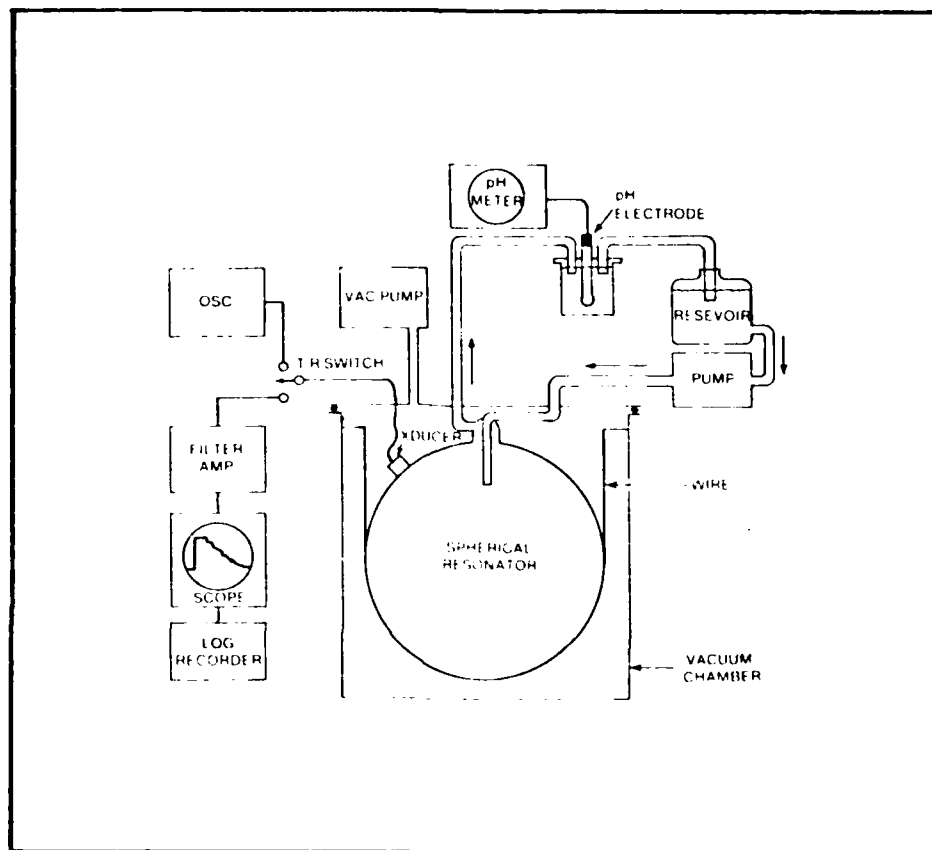


Figure 2-4. Schematic of Resonator Apparatus

A PZT cylinder, 3.8 cm in length and diameter, serves as a transducer for both the acoustic measurements and degassing the liquid. With the flask almost completely filled with distilled water, excess dissolved gas is removed by boiling at reduced pressure. Cavitation induced by driving the cylinder at its 60 kHz resonance, helps speed up the process.

The reservoir is also degassed initially at reduced pressure, and also while dissolving chemicals which may contain occluded gases. Accidental removal of desired  $\text{CO}_2$  is avoided by omitting this step, unless the pH is well above 7 where ionization is nearly complete.

In the measurement mode, the liquid is at atmospheric pressure while pressure in the vacuum chamber is reduced to less than 1 mm Hg. The resonator is excited at a selected frequency by a pulse of a few seconds duration which allows the sound field to reach equilibrium. The driver used for this purpose is a 60 W amplifier capable of producing 100 V rms across the load up to frequencies in excess of 100 kHz. A signal generator of the frequency synthesizer type is required for stability. A tone-burst generator is used to control the duration of the pulse and the time delay between pulses.

After the excitation pulse, the transducer is automatically switched from transmit to receive by means of a T/R relay. The receiver system consists of a low-noise preamplifier and a tuneable bandpass filter. The output of the filter is fed to a storage oscilloscope so that the signal decay can be monitored during the tuning procedure. Measurement of the decay rate is by means of a logarithmic graphic recorder with 50 dB range. For convenience in comparing resonator measurements with sea data, the measured values are converted from dB/sec to dB/km by dividing by the nominal sound speed 1.5 km/sec.

Finding the resonances is a very tedious process. Because the "sphere" is far from ideal, calculation of resonant frequencies is generally impractical and they must be located by searching. At the lower frequencies, the Q may be so high that the frequency cannot be stepped more than 1 Hz at

a time; otherwise, a resonance may be missed entirely. At higher frequencies, bigger steps are possible, but the range to be covered is greater and takes a long time to cover.

Care must also be taken when adding chemicals because the sound speed increases causing the resonant frequencies to increase. Measurement of the shift at the lowest frequency and calculation of the larger shifts at higher frequencies is an effective means of following the changes.

Certain resonances may become unusable or even lost and others must be found to replace them. The main reason for this difficulty is mode-coupling, a problem that has not been extensively discussed in the earlier work. When resonances involve more than one mode, interference effects can be troublesome. If the frequency spacing is great enough, the decay curve may oscillate. If one mode then decays more slowly and the oscillations die out, the data may be usable. However, if the modes are closely spaced and of comparable decay rate, the decay will appear to be linear but the slope can change with small changes in sound speed. Such changes in residual loss seriously affect the accuracy of measurements, particularly at the lower frequencies where mode interference is the primary source of error.

Various procedures can be effective in alleviating the mode problem. Absorption can be increased by increasing concentrations up to the point where other problems arise (precipitation, polymerization, etc.). For pH-dependent relaxations, losses may also be increased by increasing pH above the normal range. In addition, the residual losses can be checked by reducing pH to the point where the chemical losses become negligible. If the residual loss changes excessively, the measurement can be rejected and the procedure continued, altering the conditions slightly until repeatable results are obtained.

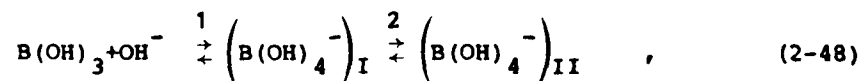
The lowest two radial modes of the resonator are too lossy to be of use. The lowest usable resonance in all cases appears to correspond to

the third mode. For the 72-liter sphere, the corresponding frequency is nominally 12 kHz. The highest usable frequency is governed by viscous losses which increase rapidly above 100 kHz making the resonances difficult to find. The same problem may also arise at the lower frequencies if the chemical loss becomes too large. Combination of all these factors results in a measurement window of limited range in both frequency and absorption coefficient. The absorption spectrum must fall within the window, if the relaxation process is to be analyzed.

The accuracy of the resonator method is difficult to access. At the lowest resonance, the residual loss is roughly 2 dB/km. Incremental changes as low as 0.2 dB/km can probably be measured with acceptable accuracy, but only after considerable repetition and averaging. Near 100 kHz, residual plus H<sub>2</sub>O losses increase to roughly 6 dB/km and the minimum limits are correspondingly greater. Estimates of relaxation frequency and  $\alpha_{\max}$  involve averaging over the 10 - 100 kHz range, but errors at the higher frequencies tend to dominate and the accuracy is not significantly improved over the low-frequency value. A rough estimate of the rms error might be  $\pm 10$  percent for  $\alpha_{\max}$  in the range 2 - 20 dB/km and also for  $f_r$  in the range 20 - 50 kHz, with rapidly increasing error outside those limits. However, possible systematic errors in the procedure may tend to bias the results. In any case, the B(OH)<sub>3</sub> values for nominal sea water conditions fall below the limits. Therefore, measurements are made at increased concentrations and compared to the sea values by extrapolation.

#### 2.4 BORIC ACID

Simmons' model for the boric relaxation in both synthetic sea water and NaCl solution is the two-step ionization equilibrium



where the slower step 2 controls the rate. Argument is based on T-jump measurements of relaxation frequency vs. concentration at pH = 8.0 (figure 2-5). Note that the relaxation frequency is always below the resonator range.

If ion-pairing is neglected, the data of figure 2-5 can be fitted by equation (2-36)

$$\omega_r = k_2^- + \frac{k_2^+ K_1 [\text{B(OH)}_3]}{1 + K_1 [\text{B(OH)}_3]} \quad (2-49)$$

The hydroxyl term  $[\text{OH}^-] \sim 10^{-6}$  M is neglected. Values of  $k_2^+$  and  $K_1$  can be determined from the data but  $k_2^-$  is too small to measure and its value must be inferred from the overall equilibrium constant  $K_1(1+K_2)$ , where  $K_2 = k_2^+ / k_2^-$ .

If the effects of ion-pairing are included, the equilibrium of equation (2-39) shows that the individual association constants of the two borate species must be known.

A second problem is what values to use for calculating  $\Delta V$ . This involves not only the association constants and their corresponding  $\Delta V$ 's, but also pH. The reason is that there is coupling to the  $\text{H}_2\text{O}$  equilibrium. The volume change for the  $\text{H}_2\text{O}$  equilibrium at 25°C is

$$\Delta V_w = v^\circ(\text{H}^+) + v^\circ(\text{OH}^-) - v(\text{H}_2\text{O}) = -4.7 + 0.5 - 18.0 = -22.2/\text{kM} \quad (2-50)$$

Measurements of the volume change for the boric acid equilibrium can be made by the pH vs. pressure method. The pertinent equilibrium constant in this case is

$$K_B = \frac{[\text{B(OH)}_4^-] [\text{H}^+]}{[\text{B(OH)}_3]} \quad (2-51)$$

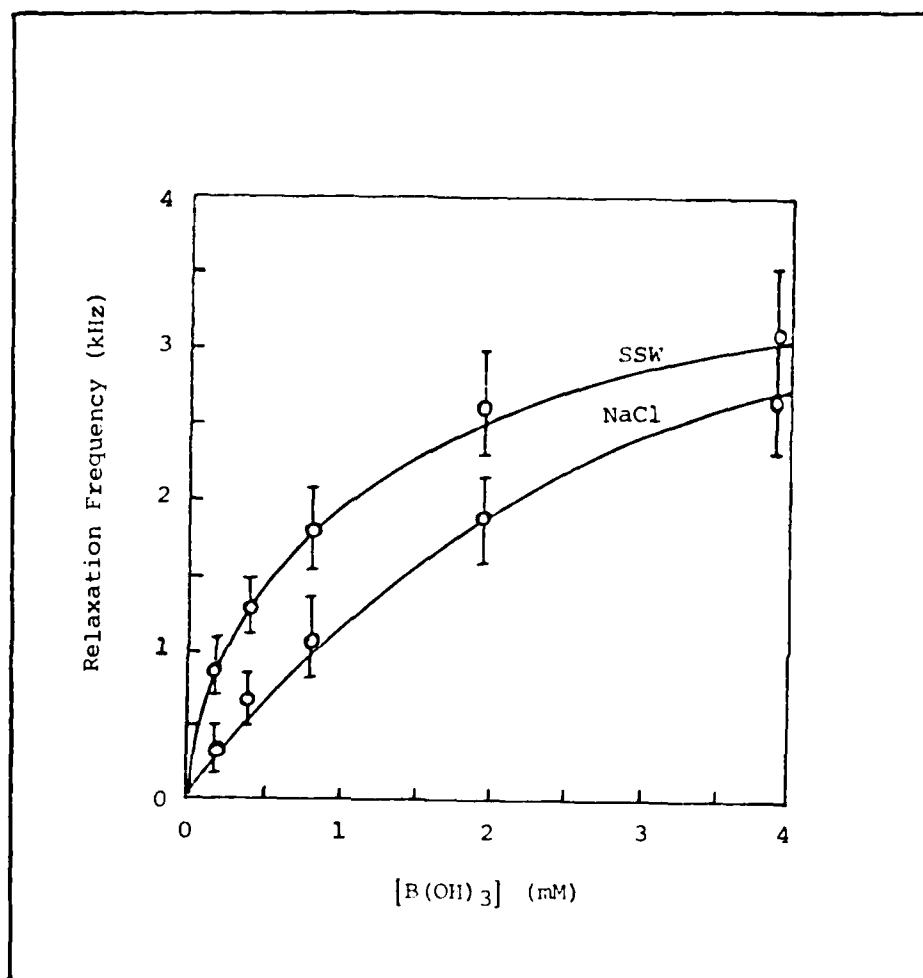


Figure 2-5. Simmons' T-jump Measurements of Relaxation Frequency vs. Concentration in Synthetic Sea Water and in 0.725M NaCl Solution

where  $[B(OH)_4^-] = [(B(OH)_4^-)_I] + [(B(OH)_4^-)_{II}]$ . The apparent volume change is calculated from the relation

$$\Delta V^* = \frac{-\partial \ln K_B}{\partial P} RT \quad (2-52)$$

The equilibrium constant for equation (2-48) is  $K_1(1+K_2)$ . Thus,  $K_B = K_w K_1(1+K_2)$ , where  $K_w = [H^+][OH^-] = 10^{-14}$ , and equation (2-52) yields

$$\Delta V^* = \Delta V_w + \Delta V_1 + \frac{K_2 \Delta V_2}{1+K_2} \quad (2-53)$$

The estimated values for aqueous solution at 25°C are  $\Delta V^* = -35.5/\text{kM}$  and  $\Delta V_w = -22.2/\text{kM}$ . With  $K_2 \gg 1$ , we then have  $\Delta V_1 + \Delta V_2 = -13.3/\text{kM}$ .

The same results are obtained by the picnometer method. The molal volumes at 25°C are  $V^{\circ}(B(OH)_3) = 39.2/\text{kM}$  and  $V^{\circ}(B(OH)_4^-) = 26.4/\text{kM}$ . Given  $V^{\circ}(OH^-) = 0.5/\text{kM}$ , we then have

$$\Delta V_1 + \Delta V_2 = V^{\circ}(B(OH)_4^-) - V^{\circ}(B(OH)_3) - V^{\circ}(OH^-) = -13.3/\text{kM} \quad (2-54)$$

Equation (2-38) with  $K_3 = [H_2O]/[H^+][OH^-] = 5.6 \times 10^{15}/M$  yields

$$\Delta V \approx \Delta V_2 + \frac{\Delta V_1 [OH^-] + \Delta V_w [H^+]}{[H^+] + [OH^-] (1 + K_1 [B(OH)_3])} \quad (2-55)$$

Now, for pH = 8.0 or greater  $[H^+] \ll [OH^-]$ , it is evident that coupling effects to the  $H_2O$  equilibrium will be negligible. At pH = 6.0 or less,  $\Delta V + \Delta V_2 + \Delta V_w$ , but absorption is negligible in that range anyway.

The effects of  $\text{NaB(OH)}_4$  ion-pairing on absorption also appear to be negligible, since  $\alpha_{\text{max}}$  is independent of NaCl concentration up to 0.4M. This shows that the slow step is unaffected by  $\text{Na}^+$  ion-pairing. The appropriate equilibrium in this case is equation (2-39) with the values  $K_3 = K_5 = 2.1/\text{M}$  and  $\Delta V_3 = \Delta V_5 = 8/\text{KM}$ . Then  $\Delta V$  is unaffected despite the large change in molal volume for  $\text{NaB(OH)}_4^{\ominus}$  formation.

The relaxation frequency obtained from equation (2-40) with  $[\text{Na}^+] \gg [\text{B(OH)}_4^-]$ , is

$$\omega_r = k_2 + \frac{k_2^+ K_1 [\text{B(OH)}_3] (1 + K_{\text{NaB}} [\text{Na}^+])}{1 + K_1 [\text{B(OH)}_3] (1 + K_{\text{NaB}} [\text{Na}^+])} \quad (2-56)$$

The only effect is that  $K_1 (1 + K_{\text{NaB}} [\text{Na}^+])$  appears in place of  $K_1$ . This indicates that the apparent equilibrium constant of boric acid in NaCl solution should be used in calculating  $k_2^-$ . In addition, ion-pairing of  $\text{NaOH}^{\ominus}$  should not be neglected because the ionization constant of water changes significantly in NaCl solution. By similar arguments, we can show that the apparent equilibrium constant of  $\text{H}_2\text{O}$  should also be used in the calculations. Table 2-2 lists the calculated values based on these assumptions.

Table 2-2.  $\text{B(OH)}_3$  Rate and Equilibrium Constants Calculated Using Apparent Constants  $\text{pK}_w^* = 13.77$  and  $\text{pK}_B^* = 8.83$  With Estimated Diffusion-Control Value for  $k_1^+$  (Simmons Theory)

NaCl	SSW
$K_1^* = 5.6 \times 10^2/\text{M}$	$K_1^* = 1.6 \times 10^3/\text{M}$
$k_1^+ = 3 \times 10^{10}/\text{M}\cdot\text{s}$	$k_1^+ = 3 \times 10^{10}/\text{M}\cdot\text{s}$
$k_1^- = 1.4 \times 10^8/\text{s}$	$k_1^- = 4.2 \times 10^7/\text{s}$
$K_2 = 154$	$K_2 = 53$
$k_2^+ = 2.5 \times 10^4/\text{s}$	$k_2^+ = 2.2 \times 10^4/\text{s}$
$k_2^- = 1.6 \times 10^2/\text{s}$	$k_2^- = 4 \times 10^2/\text{s}$

In equation (2-54),  $\Delta V_1$  and  $\Delta V_2$  cannot be differentiated by absorption measurements because at the concentration where  $\alpha_{\max}$  can be measured accurately, the effect of  $\Delta V_1$  is very small. Simmons proposes that the intermediate state is a contact ion-pair with negligible volume change and that all of the  $\Delta V$  arises from the second step. This is consistent with other evidence that a change from trigonal planar to tetragonal symmetry is involved in the ionization of boric acid<sup>29</sup> and this may be the rate-controlling process.

Measurements of  $\alpha_{\max}$  vs. concentration are compared with theory in figure 2-6. The constituent used in this case is  $\text{Na}_2\text{B}_4\text{O}_7 \cdot 10\text{H}_2\text{O}$  (borax). The theoretical curve is for Simmons' model.

Figure 2-7 compares measurements of  $\alpha_{\max}$  as a function of pH for borax and boric acid. A possible reason for the anomalous pH behavior of borax is that a stable aquo-complex may persist which inhibits absorption at high pH (equation 2-8). The pH dependence of boric acid is normal, but the magnitude is too large.

Despite the obvious disagreement between theory and experiment, some conclusions can be made. Note that the measured value of  $\alpha_{\max}$  at pH = 8.0 is roughly twice that of sea water while the concentration is some 20 times greater. At lower concentrations, absorption becomes too small to measure, except at higher pH values where the lowest measureable concentration is roughly 5 times sea water. Extrapolation to sea water conditions shows that  $\alpha_{\max}$  is more than an order of magnitude too low.

## 2.5 SYNTHETIC SEA WATER

For  $\text{B}(\text{OH})_3$  absorption measurements in synthetic sea water, it is desirable to eliminate all other relaxations that cause additional absorption in the measurement range. This can be done by omitting certain constituents. However, coupling between equilibria may change and this could affect the  $\text{B}(\text{OH})_3$  relaxation.

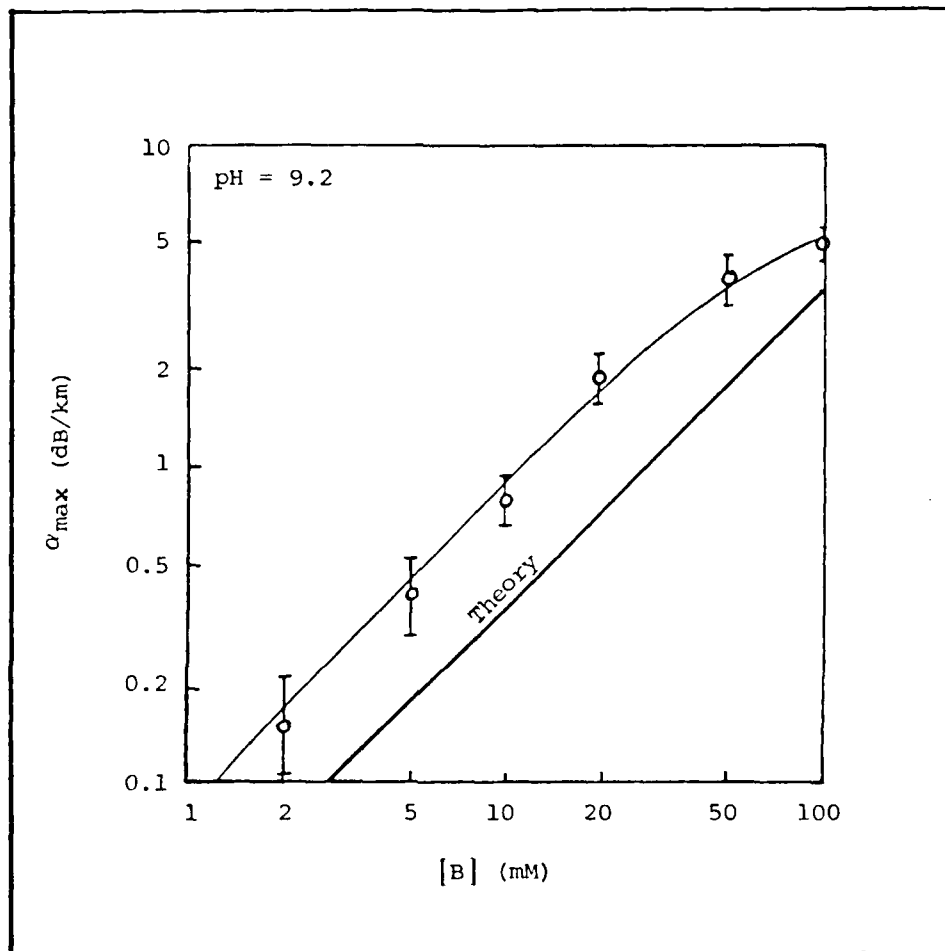


Figure 2-6. Resonator Measurements of  $\alpha_{\max}$  vs. Concentration in Aqueous  $B(OH)_3$  Compared to Theory

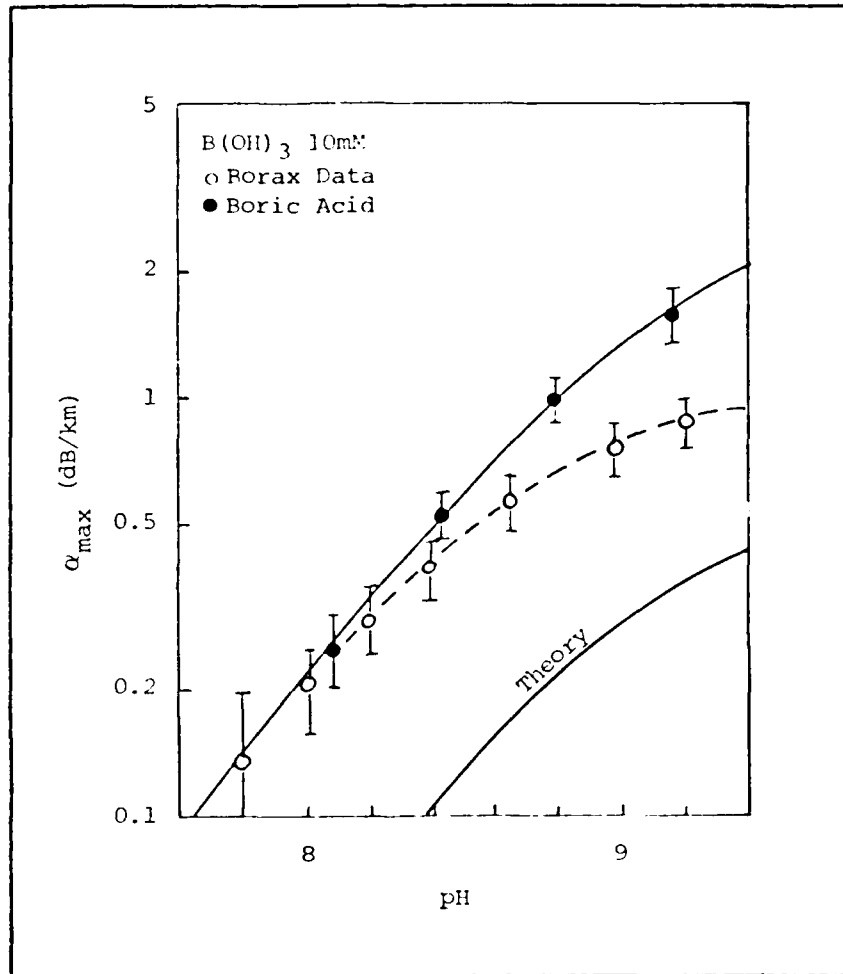


Figure 2-7. Resonator Measurements of  $\alpha_{\max}$  vs. pH in Aqueous  $B(OH)_3$  Compared to Theory

Sulfate will be omitted with no apparent effect other than elimination of the  $\text{MgSO}_4$  relaxation which would otherwise dominate absorption in the 10 - 100 kHz range. Magnesium is also involved in the  $\text{MgCO}_3^0$  and  $\text{MgB(OH)}_4^+$  relaxations, both of which produce considerable absorption in this range. The effects of omission also appear to be small. The only constituents in addition to  $\text{B(OH)}_3$  that are necessary to approximate the essential sea water conditions are then  $\text{CaCl}_2$  and  $\text{NaHCO}_3$ . However,  $\text{NaCl}$  may be useful to stabilize carbonate activity.

The T-jump measurements showed that  $\text{NaHCO}_3$  causes an increase in the  $\text{B(OH)}_3$  relaxation frequency, while other constituents tend to reverse this effect. As in aqueous solution, the relaxation frequency never exceeds 4 kHz under any conditions.

The effects of  $\text{CO}_2$  on the  $\text{B(OH)}_3$  absorption spectrum in 0.4 M  $\text{NaCl}$  solution are shown in figure 2-8. At the highest concentration, the measured relaxation frequency is roughly 20 kHz. Initially, this was believed to be another relaxation because the relaxation frequency exceeds the T-jump maximum. The first experiments involved  $\text{NaCl}$  solution, and an ion-pairing relaxation was suspected. However, attempts to match the spectra with a two-relaxational model were not successful. Subsequent experiments showed high relaxation frequencies without additional  $\text{NaCl}$ . Here the results are difficult to analyze because of changes in carbonate activity. However, the spectra appear to be almost identical in both 0.1 M and 0.4 M  $\text{NaCl}$  solutions. In addition, similar results are observed when  $\text{CaCl}_2$  is substituted for  $\text{NaCl}$ . The observed relaxation is clearly the sea water one, the higher relaxation frequency being simply the result of increased concentrations. The discrepancy with T-jump measurements can be explained, if pH and absorption are controlled by different relaxations under certain conditions.

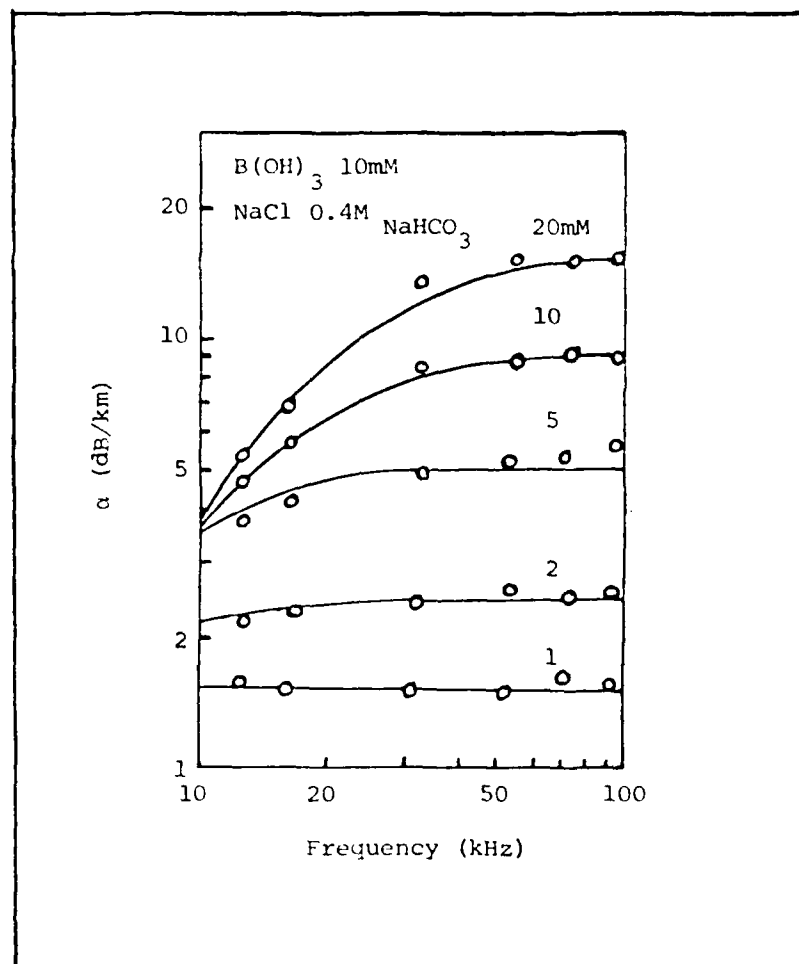


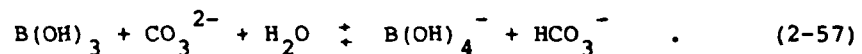
Figure 2-8.  $\text{B(OH)}_3$  Absorption Spectra in  $\text{Na/CO}_2$  System as a Function of  $\text{NaHCO}_3$  Concentration at  $\text{pH} = 9.0$

Figure 2-9 shows the absorption spectra with  $\text{CaCl}_2$  substituted for  $\text{NaCl}$ . In this experiment, the  $\text{NaHCO}_3$  concentration is reduced to 0.4X (0.4 times the sea water value) to prevent  $\text{CaCO}_3$  precipitation at high pH. The absorption spectra are then measured for various total  $\text{B(OH)}_3$  concentrations.

In both experiments, the relaxation frequency is approximately a linear function of the varied concentration. Extrapolated to sea water concentrations, the relaxation frequency is approximately equal to the ocean value  $f_r \approx 1$  kHz.

Now  $\alpha_{\text{max}}$  also increases linearly with either concentration. Values of  $\alpha_{\text{max}}$  in  $\text{NaCl}$  solution corrected for concentration and pH to sea water conditions are an order of magnitude too small. However, with  $\text{CaCl}_2$ , agreement is good. It is apparent, therefore, that the omitted constituents play only a minor role in the  $\text{B(OH)}_3$  relaxation.

Linear dependence of relaxation frequency on the sum of concentrations and product dependence of  $\alpha_{\text{max}}$  indicates the exchange equilibrium,



For the exchange equilibrium, we have from equation (2-42)

$$\omega_r = k^+ \left( \left[ \text{B(OH)}_3 \right] + \left[ \text{CO}_3^{2-} \right] \right) + k^- \left( \left[ \text{B(OH)}_4^- \right] + \left[ \text{HCO}_3^- \right] \right) \quad (2-58)$$

$$\alpha_{\text{max}} = \frac{(\Delta V)^2 k^+ \left[ \text{B(OH)}_3 \right] \left[ \text{CO}_3^{2-} \right] \rho_{\text{O}_2\text{CO}}}{2RT}$$

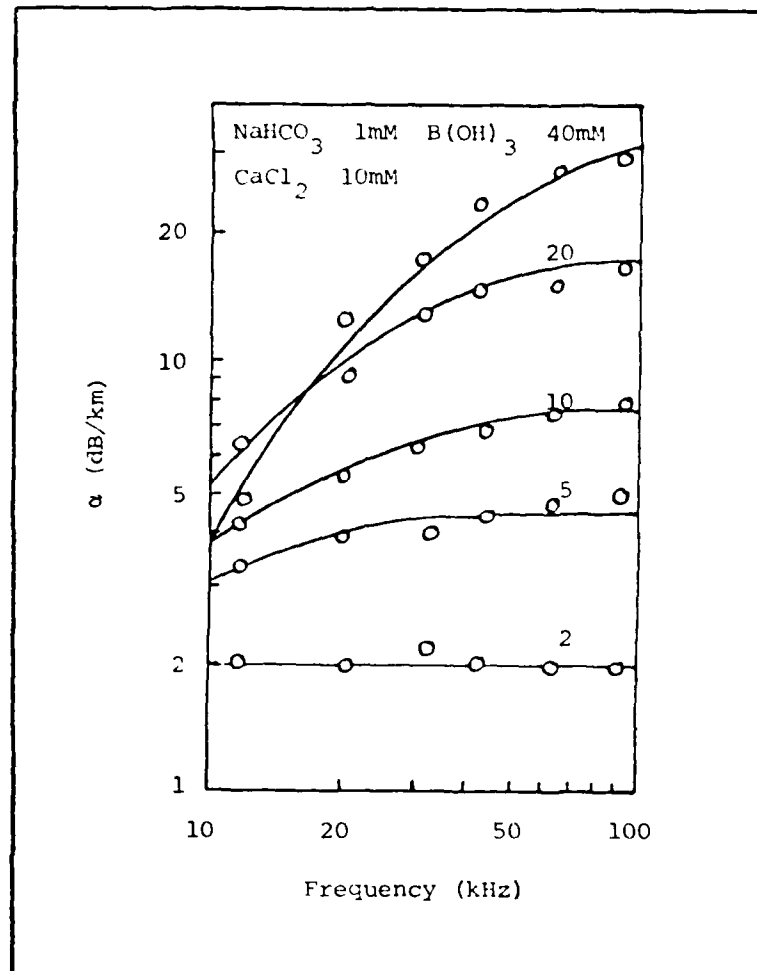
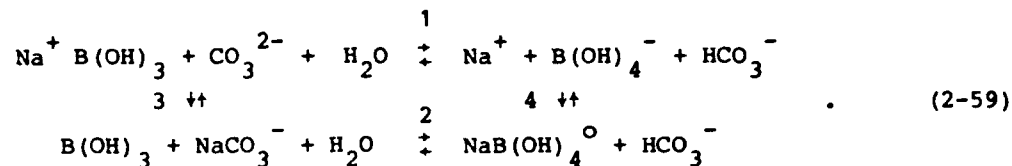


Figure 2-9. B(OH)<sub>3</sub> Absorption Spectra in Ca/CO<sub>2</sub> System  
as a Function of B(OH)<sub>3</sub> Concentration at pH = 9.1

The reason for the negligible effect of  $\text{Na}^+$  ion-pairing is apparently the same as proposed for aqueous solution, i.e., the rates,  $\Delta V$ 's and association constants are similar for both reaction paths. The suggested exchange scheme in  $\text{NaCl}$  solution is



For  $[\text{Na}^+] \gg [\text{B(OH)}_4^-], [\text{CO}_3^{2-}]$  in equation (2-44),

$$\begin{aligned} \omega_r \approx k_1^+ & \left( \frac{[\text{B(OH)}_3]}{1 + K_3[\text{Na}^+]} + [\text{CO}_3^{2-}] + \frac{1}{K_1} \left( [\text{B(OH)}_4^-] + \frac{[\text{HCO}_3^-]}{1 + K_4[\text{Na}^+]} \right) \right) \\ & + k_2^+ \left( \frac{K_3^- [\text{Na}^+] [\text{B(OH)}_3]}{1 + K_3[\text{Na}^+]} + [\text{CaCO}_3^0] + \frac{K_3[\text{Na}^+]}{K_1} \left( [\text{B(OH)}_4^-] + \frac{[\text{HCO}_3^-]}{1 + K_4[\text{Na}^+]} \right) \right) \end{aligned} \quad (2-60)$$

$$\Delta V = \Delta V_1 - \frac{\Delta V_3 K_3 [\text{Na}^+]}{1 + K_3 [\text{Na}^+]} + \frac{\Delta V_4 K_4 [\text{Na}^+]}{1 + K_4 [\text{Na}^+]}$$

In this case, the forward rate is independent of  $[\text{Na}^+]$ , if  $k_1^+ = k_2^+$ . The reverse rates cannot then be equal because  $K_3 > K_4$ , and  $k_1^-/k_2^- = K_4/K_3$ . For calculations, the values used are  $K_1 = 4$ ,  $K_3 = 1.6/\text{M}$ ,  $K_4 = 2.1/\text{M}$ ,  $\text{pK}_B^* = 9.0$ , and  $\text{pK}_{2C}^* = 9.6$ . Assuming  $k_1^+ = k_2^+$ , the relaxation frequency can be written  $\omega_r = k^+ \times$  effective concentration. The value of  $k^+$  estimated by fitting the data of figure 2-10 is  $7.5 \times 10^6/\text{M}\cdot\text{s}$ .

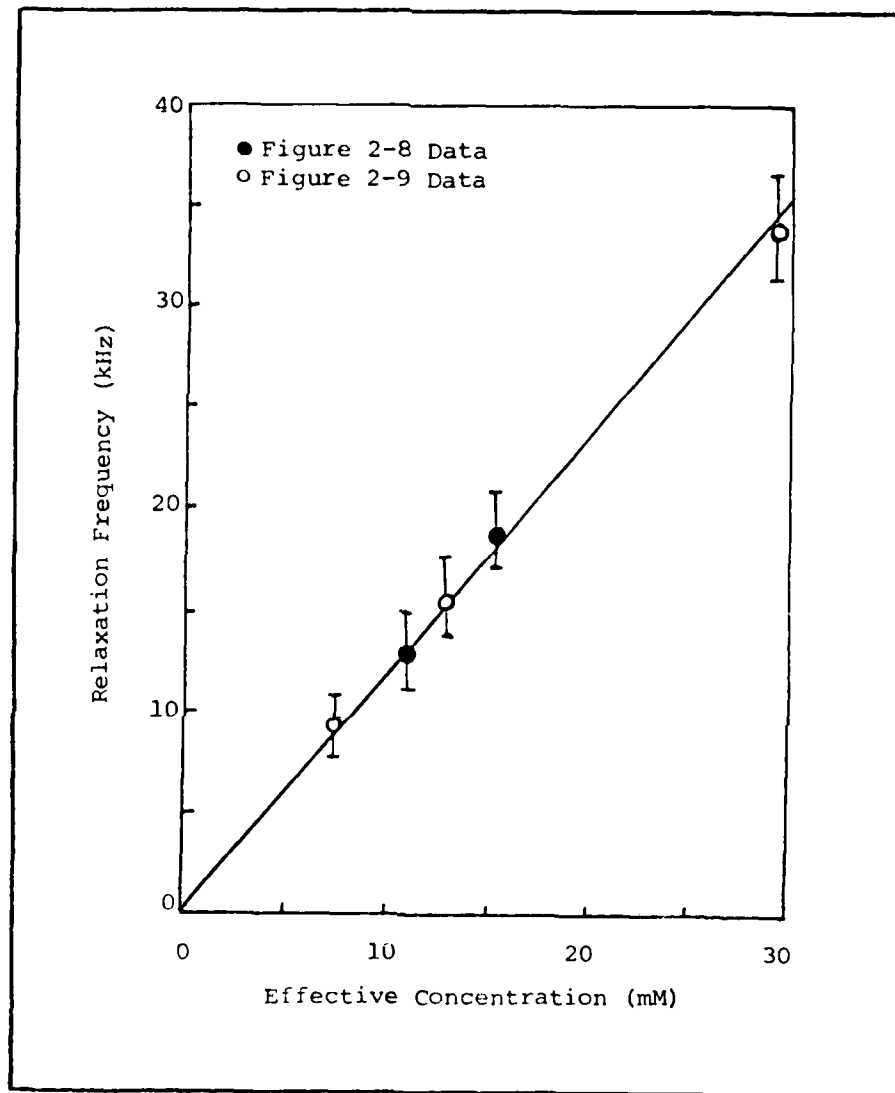


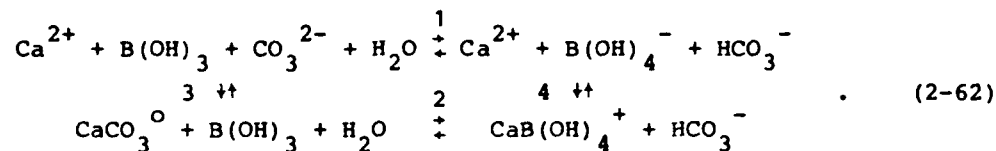
Figure 2-10. Relaxation Frequency vs. Effective Concentration

In figure 2-11, the  $\alpha_{\max}$  data are plotted vs. the concentration product  $[B(OH)_3] \times [\Sigma CO_3^{2-}]$ . The value of  $\Delta V$  is calculated by curve-fit. In NaCl solution,  $\Delta V = -7/kM$ . The value for the exchange is

$$\Delta V = v^{\circ}(B(OH)_4^-) + v^{\circ}(HCO_3^-) - v^{\circ}(B(OH)_3) - v^{\circ}(CO_3^{2-}) - v(H_2O) = -8.2/kM. \quad (2-61)$$

In equation (2-60), we then have  $\Delta V_1 = -8.2/kM$ ,  $\Delta V_3 = 12/kM$ , and  $\Delta V_4 = 8/kM$ . The calculated value is then  $\Delta V = -7.4/kM$ , which is in good agreement with the measured value.

In  $CaCl_2$  solution, the curve-fit value is  $\Delta V = -21/kM$ . The scheme for  $CaCl_2$  is



In this case, the approximation  $[Ca^{2+}] \gg [B(OH)_4^-]$ ,  $[CO_3^{2-}]$  is not accurate and the exact equations are used. For calculation purposes, the values are  $pK_B^* = 9.1$ ,  $pK_{2C}^* = 9.7$ ,  $K_4 = 26/M$  and  $K_3 = 125/M$ . For  $\Delta V_4 = 0$  and  $\Delta V_3 = 12.5/kM$ , the calculated value is  $\Delta V = -16/kM$ , which is significantly too low in magnitude. The likely explanation is that  $K_3$  is much larger than the sea value at the lower ionic strength, making  $\Delta V = \Delta V_1 - \Delta V_3 = -20.7/kM$ , which is in good agreement with the measured value. In any case, the strong effect of  $Ca^{2+}$  is clearly due to the asymmetry in the association constants and  $\Delta V$ 's of the two  $Ca^{2+}$  ion-pairs.

In figure 2-12, the pH dependence of  $\alpha_{\max}$  is compared with theory. From equation (2-58), we have

$$\alpha_{\max} = k^+ [B] \left[ CO_2 \right] \frac{1}{1+x} \frac{y}{1+y} \quad (2-63)$$

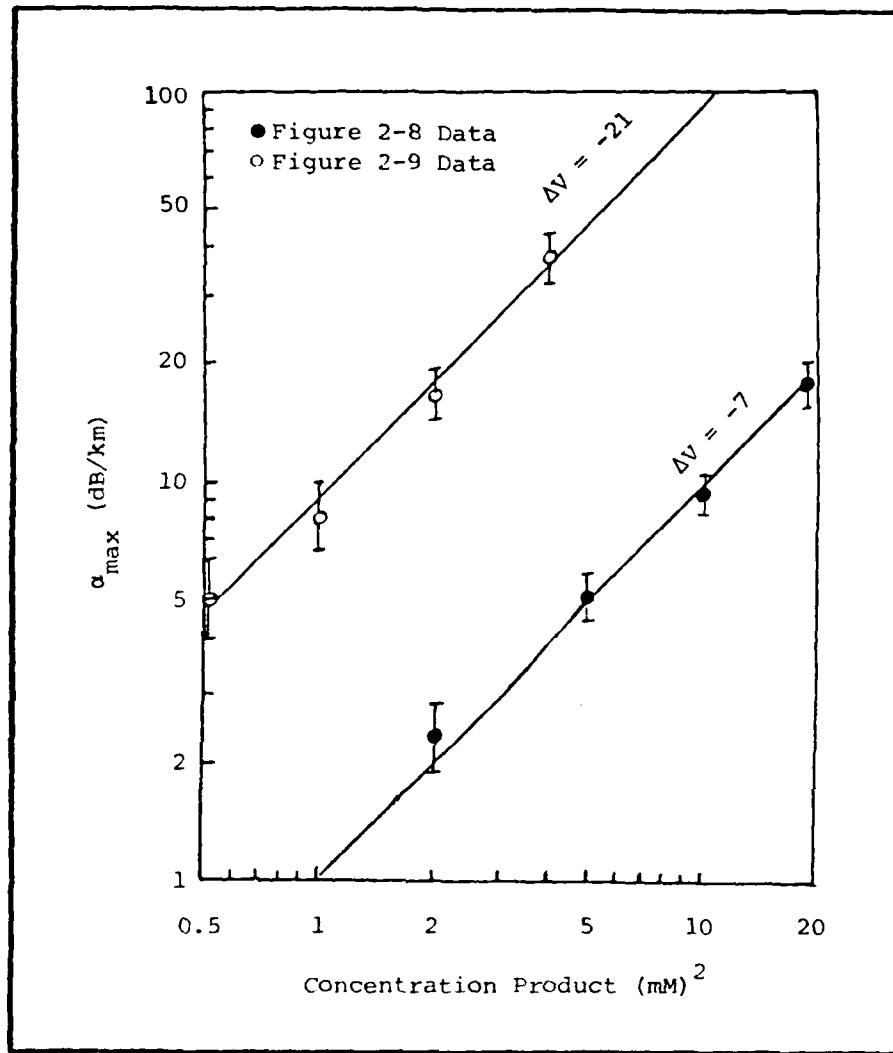


Figure 2-11.  $\alpha_{\max}$  vs. Concentration Product Compared With Theory

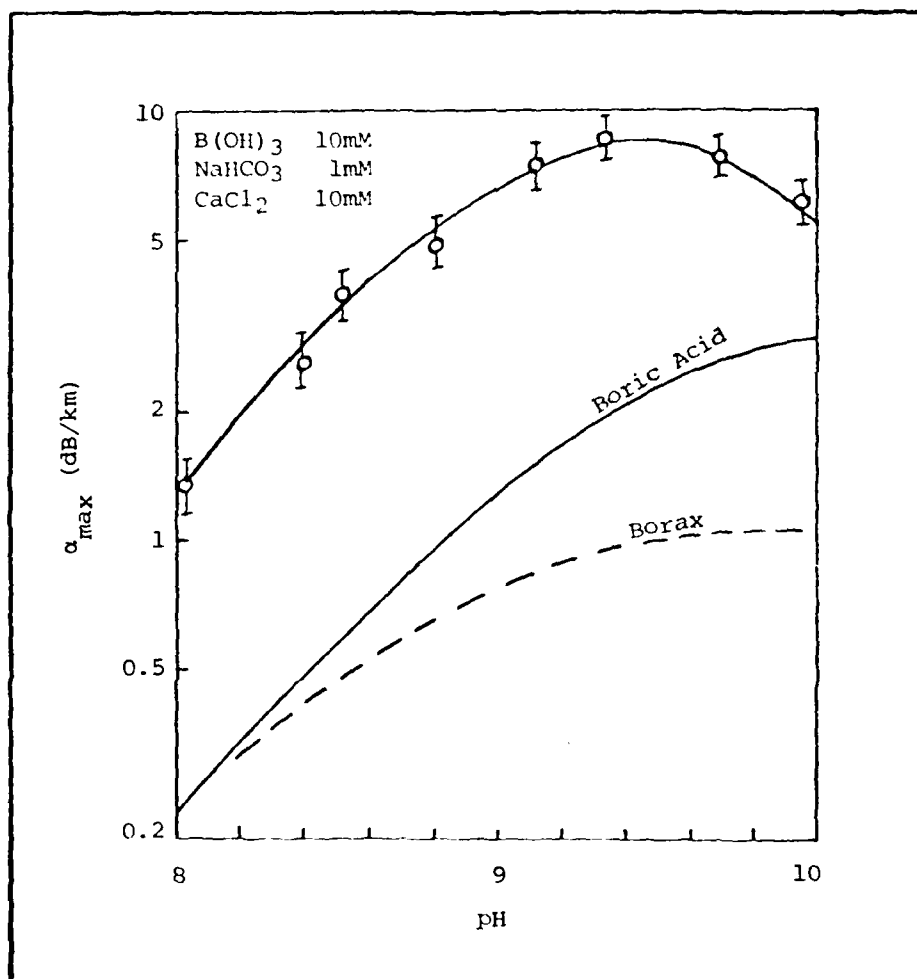


Figure 2-12.  $\alpha_{\max}$  vs. pH in  $B(OH)_3/CO_2/Ca$  System Compared With Aqueous Boric Acid and Borax Results of Figure 2-7

where  $[B]$  and  $[CO_2]$  are total concentrations,  $x = 10^{pH-pK_B^*}$ , and  $y = 10^{pH-pK_{2C}^*}$ . Agreement is taken as further support of the exchange equilibrium as the dominant mechanism in sea water.

In sea water, the effects of  $Na^+$  tend to cancel out. The same appears to be true of  $Mg^{2+}$ . However, it is more difficult to demonstrate because two additional ion-pair relaxations must be considered. Figure 2-13 shows the absorption spectrum of the  $B(OH)_3/CO_2/Mg/Ca$  system at  $pH = 8.5$ . All concentrations are sea water values, except  $B(OH)_3$ , which is 4.6X. Reduced  $NaHCO_3$  concentration is no longer necessary to prevent precipitation of  $CaCO_3$  because competitive  $MgCO_3^0$  ion-pairing keeps the concentration from becoming excessive. The solid lines represent the estimated spectra of the three component relaxations  $B(OH)_3$ ,  $MgCO_3^0$  and  $MgB(OH)_4^+$  (reference 23).

Figure 2-14 shows the calculated pH dependence of the three components. The data points are 12 kHz measurements with the other components subtracted to estimate the  $B(OH)_3$  values. The curve fit, extrapolated to sea water concentration, is about 25 percent too high, which indicates that Mg causes an increase in  $\alpha_{max}$ . A detailed analysis of the interaction is difficult because the  $MgB(OH)_4^+$  relaxations are also slow and coupling effects are not easily estimated when the rates are comparable.

In figures 2-15 and 2-16, the pH dependence of the full SSW system is examined at two widely different temperatures. Analysis of sea data (reference 18) showed that  $B(OH)_3$  absorption data can be expressed in terms of  $f_r$  as a function of temperature only, and  $(\alpha\lambda)_{max}$  as a function of pH only. Thorp's values at  $T = 4^\circ C$  and  $pH = 8.0$  are used as reference and the empirical formula can be written

$$f_r = 1 \times 10^{(T-4)/100} \text{ kHz} \quad (2-64)$$

$$\alpha_{max} = 0.1 \times 10^{(pH-8)} f_r \text{ dB/km} ,$$

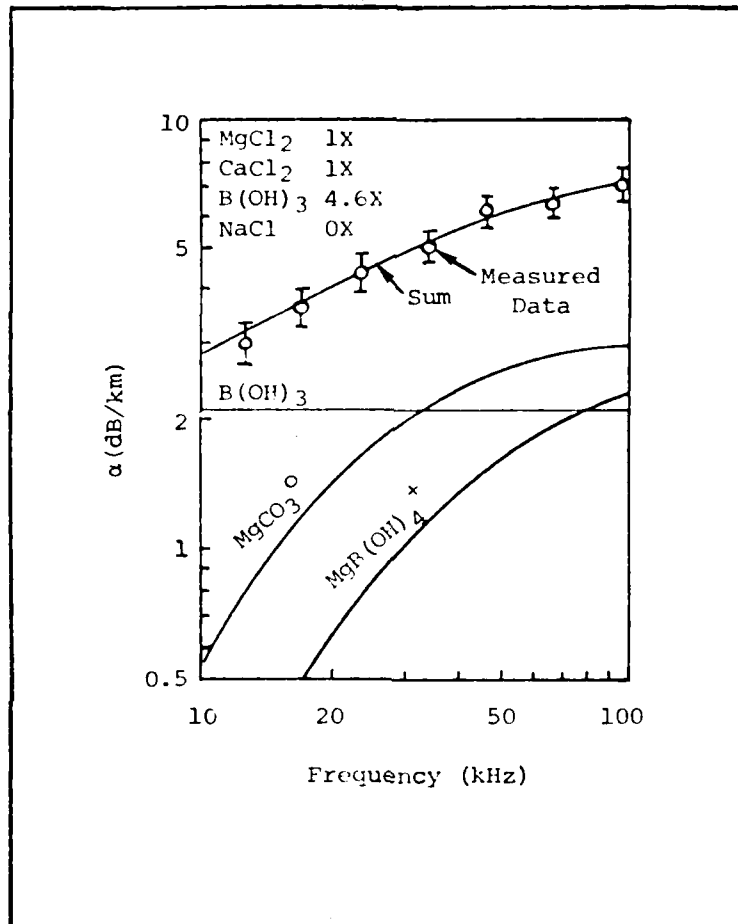


Figure 2-13.  $B(OH)_3$  Absorption Spectrum in SSW With 4.6 X  $B(OH)_3$  Concentration and  $NaCl$  Omitted Showing the Estimated Three Relaxation Components (Without  $Ca$ , the  $B(OH)_3$  component is estimated to be lower by roughly a factor of 10.)

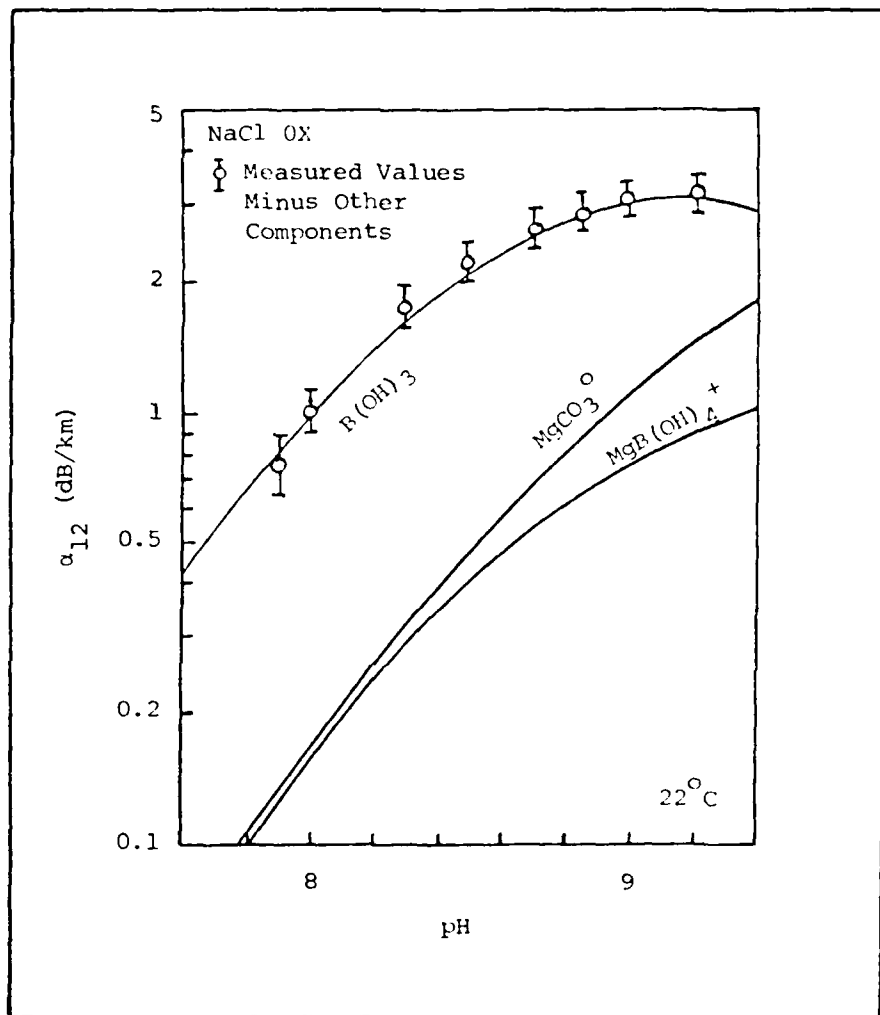


Figure 2-14. Absorption at 12 kHz vs. pH Estimated for the Three Components of Figure 2-13 (NaCl is omitted; values are  $pK_B^*$  8.92,  $pK_{2C}^*$  9.21.)

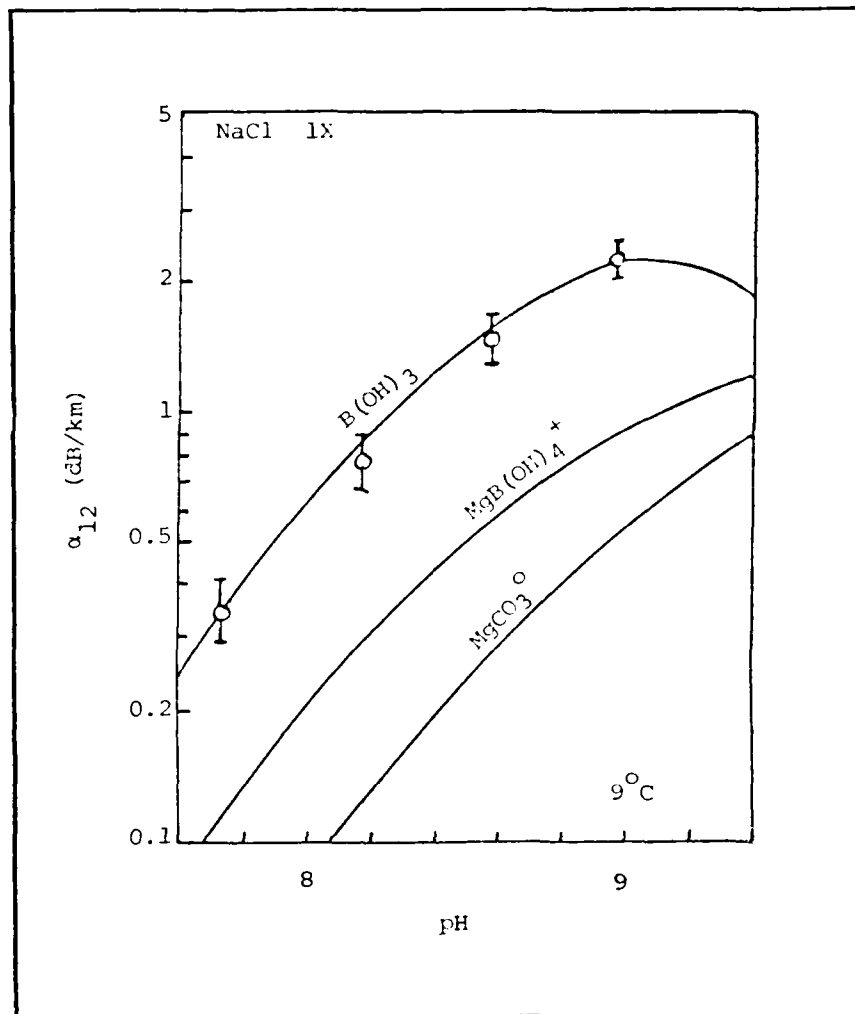


Figure 2-15. Absorption vs. pH at 12 kHz Estimated for the Three Relaxation Components at 9°C (NaCl is included; values are  $pK_B^*$  8.85,  $pK_{2C}^*$  9.28.)

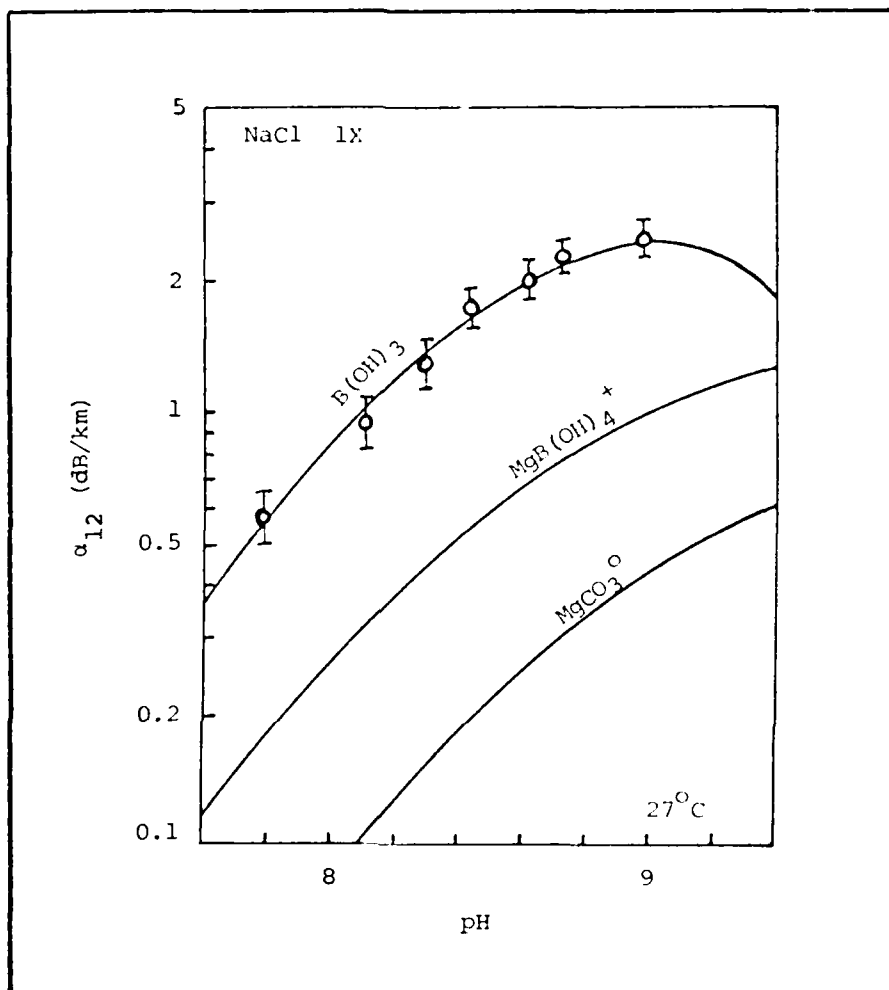


Figure 2-16. Absorption vs. pH at 12 kHz Estimated for the Three Relaxation Components at 27°C (NaCl is included; values are  $pK_B^*$  8.90,  $pK_{2C}^*$  9.05.)

where the nominal pH range is 7.8 - 8.2. Linear regression analysis of the same data by Schulkin and Marsh<sup>30</sup> and by Lovett<sup>31</sup> yielded a coefficient for the pH exponent somewhat less than unity which would account for small deviations from the asymptotic value in this range.

For comparison of the formula values with the results of figures 2-16 and 2-17, the coefficients are multiplied by 4.6 to correct for the increased  $B(OH)_3$  concentration. At 9°C and pH = 8.0, the curve-fit value of figure 2-16 is 0.57 dB/km and the model value is 0.52 dB/km. At 27°C, the corresponding values are 0.78 and 0.79 dB/km. Obviously, such excellent agreement is somewhat fortuitous, since errors of more than 10 percent might easily be expected.

The linear approximation for  $(\alpha\lambda)_{\max}$  vs.  $10^{pH}$  becomes inaccurate at high values of pH. In figure 2-17, the sea data and resonator data are compared to the actual theoretical curve. The inflection point, depends on the values of  $pK_B^*$  and  $pK_{2C}^*$ , both of which depend on temperature. However, for calculation purposes, 25°C values are appropriate for the resonator measurements, while errors in the sea water temperature range are evidently not significant because  $\Delta V$  changes evidently cancel out effects of pK changes.

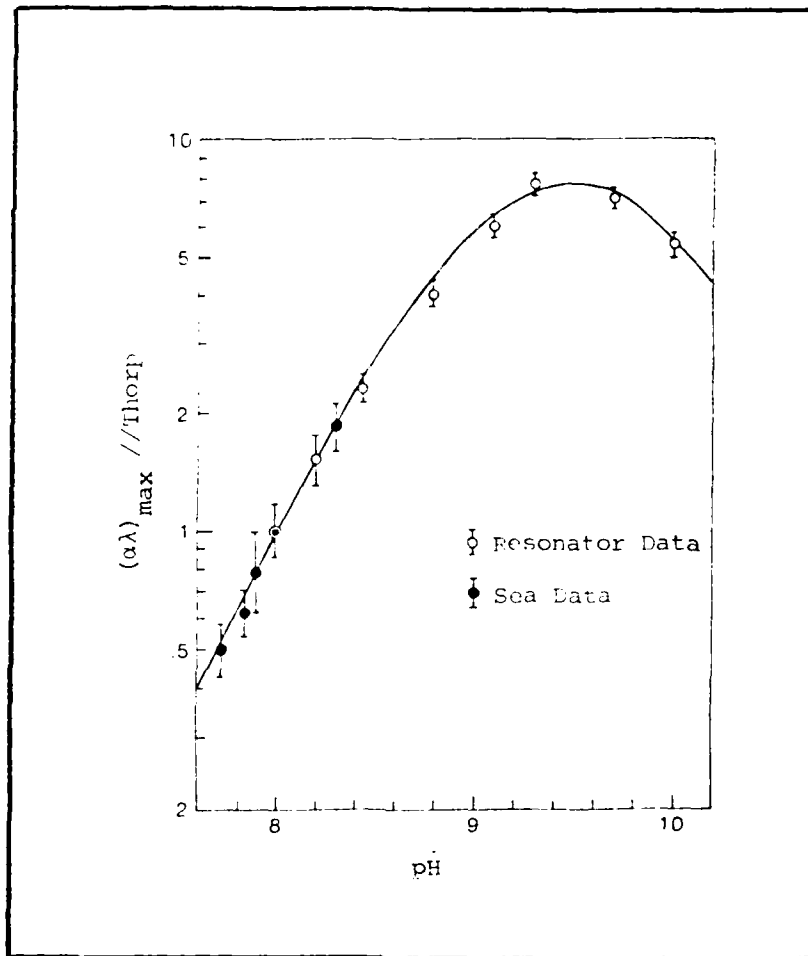


Figure 2-17.  $B(OH)_3$   $(\alpha\lambda)_{\max}$  vs. pH Relative to Thorp's Values at pH = 8.0 and 4°C Comparing Sea Data and Resonator Values

## Section 3

## DISCUSSION

The exchange model appears to give good account of  $B(OH)_3$  absorption in synthetic sea water and the ocean measurements as well. However, there are still a number of discrepancies relating to the T-jump measurements. Note that the exchange of a hydroxyl ion does not involve pH change. Thus, it is only through other coupled equilibria that absorption and T-jump measurements are related.

In figure 3-1, the relaxation vs. concentration predictions of exchange theory are compared with Simmons' SSW results. For the exchange case, relaxation frequency is a linear function of  $B(OH)_3$  concentration. The finite value, when the concentration approaches zero, is due to  $HCO_3^-$ , which is the predominant  $CO_2$  species at  $pH = 8.0$ . T-jump data agree within experimental error, except for the highest value where it appears to approach a limit as in two-step theory.

In figure 3-2, the relaxation frequency vs. pH measurements in sea water by Yeager, et al are compared with the two theories. At low pH, the relaxation frequency approaches a constant in either theory. At high pH, the relaxation frequency for exchange theory increases approaching another constant value determined by  $CO_3^{2-}$  species. Two-step theory predicts a decrease as the  $B(OH)_3$  concentration decreases. The data are in reasonable agreement with either theory, except at the highest value, where the two-step seems to give the correct trend.

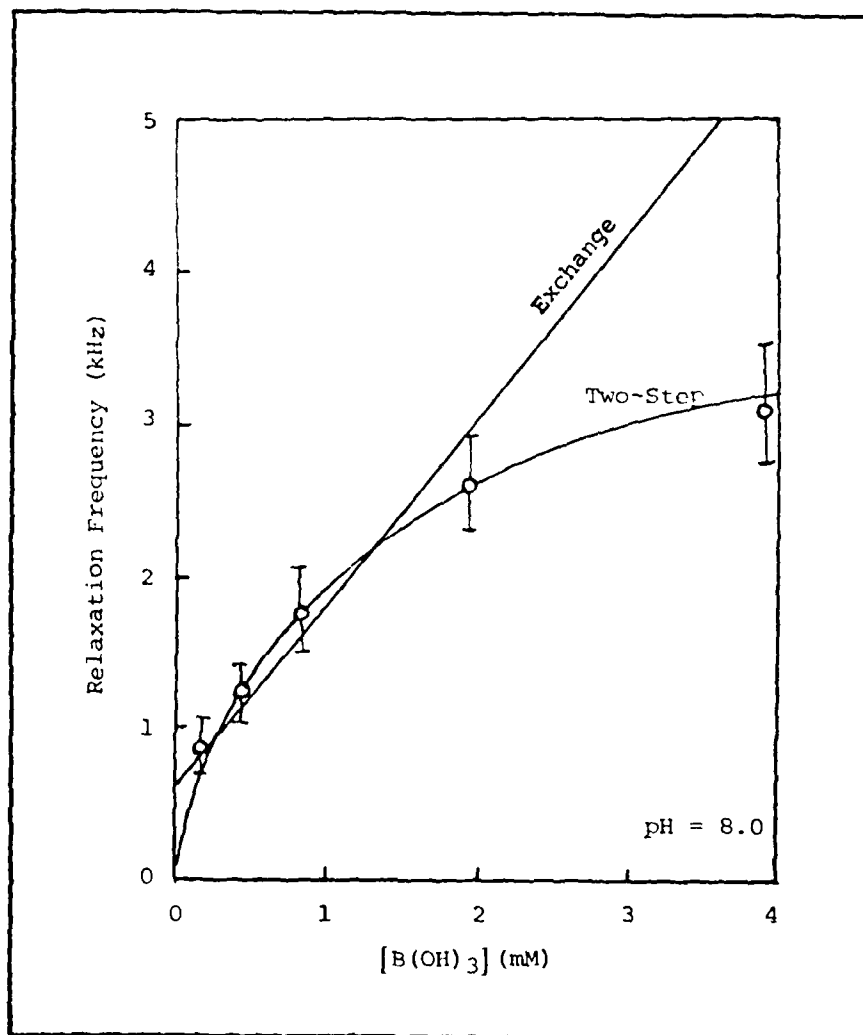


Figure 3-1. Simmons' T-jump Measurements of  $B(OH)_3$  Relaxation Frequency vs. Concentration in SSW Compared With Two-step and Exchange Theories

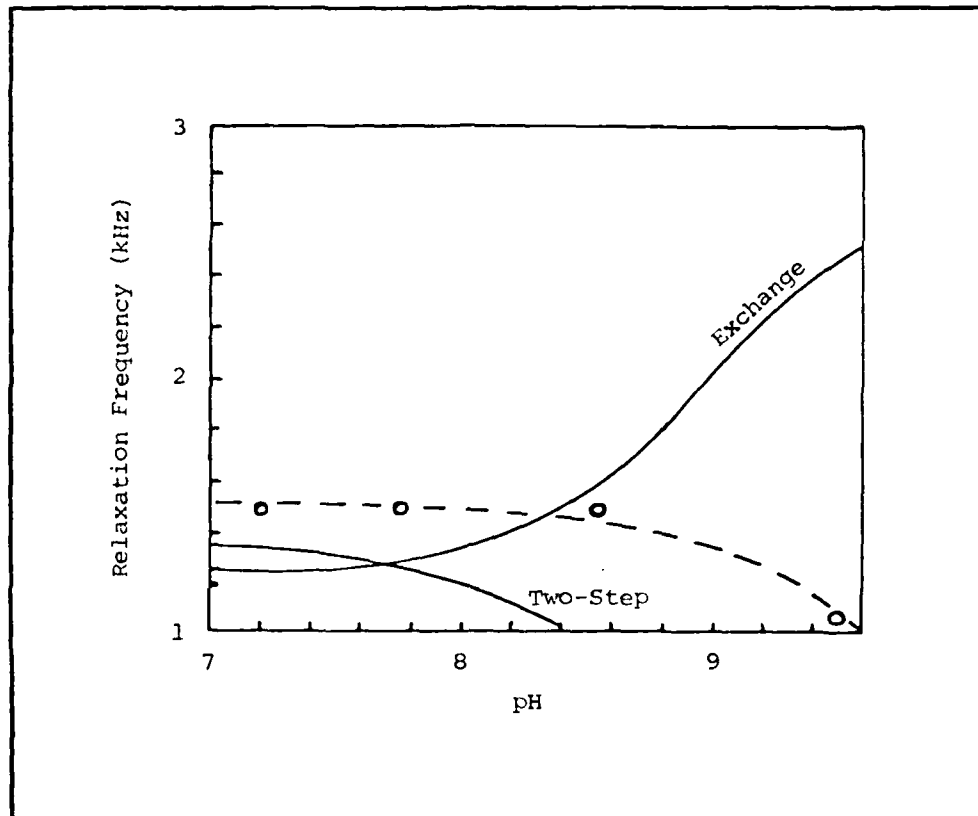
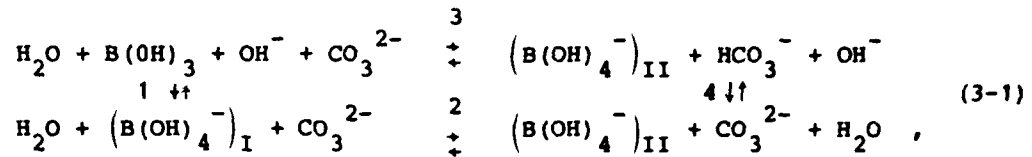


Figure 3-2. T-jump Measurements of  $B(OH)_3$  Relaxation Frequency vs. pH in Sea Water Compared With Two-step and Exchange Theories

A coupled system for the two reactions in sea water would be



where step 3 is the exchange and 1-2 is the two-step.

In a four state system, there are three eigenfrequencies. If steps 1 and 4 are both fast compared with steps 2 and 3, two are fast and the other is slow. Therefore, pH and absorption would follow the same slow relaxation, regardless of whether step 2 or 3 controls that rate. The "short circuit" would be eliminated if either steps 1 or 4 were slow also. There is no evidence for a slow relaxation in the carbonate equilibrium (step 4). However, step 1 can be slow, if the  $\text{O}^-$  association, like the exchange, is not diffusion-controlled as, Simmons assumed.

Since  $k_2^+$  places an upper limit on the two-step relaxation frequency, it is clear that the new value must be approximately the same as before. However, to fit the boric acid absorption data of figure 2-7 with the values  $\Delta V_1 = 0$  and  $\Delta V_2 = -13.3/\text{KM}$ , a much higher reverse rate is required, i.e.,  $k_2^- = 7.5 \times 10^2/\text{s}$ . The other values must be determined by curve fit to T-jump data. Approximate methods are no longer valid and the eigenfrequencies must be calculated from the roots of the determinant of equation (2-35)

$$\left| \begin{array}{cc}
 k_1^- + k_1^+ \left( [\text{B}(\text{OH})_3] + [\text{OH}^-] \right) - \omega & k_1^- \\
 k_2^+ & k_2^- + k_2^+ - \omega_r
 \end{array} \right| . \quad (3-2)$$

Curve fit of the lower mode II to the NaCl T-jump data of figure 2-5 is shown in figure 3-3. The values of the resulting rate and equilibrium constants

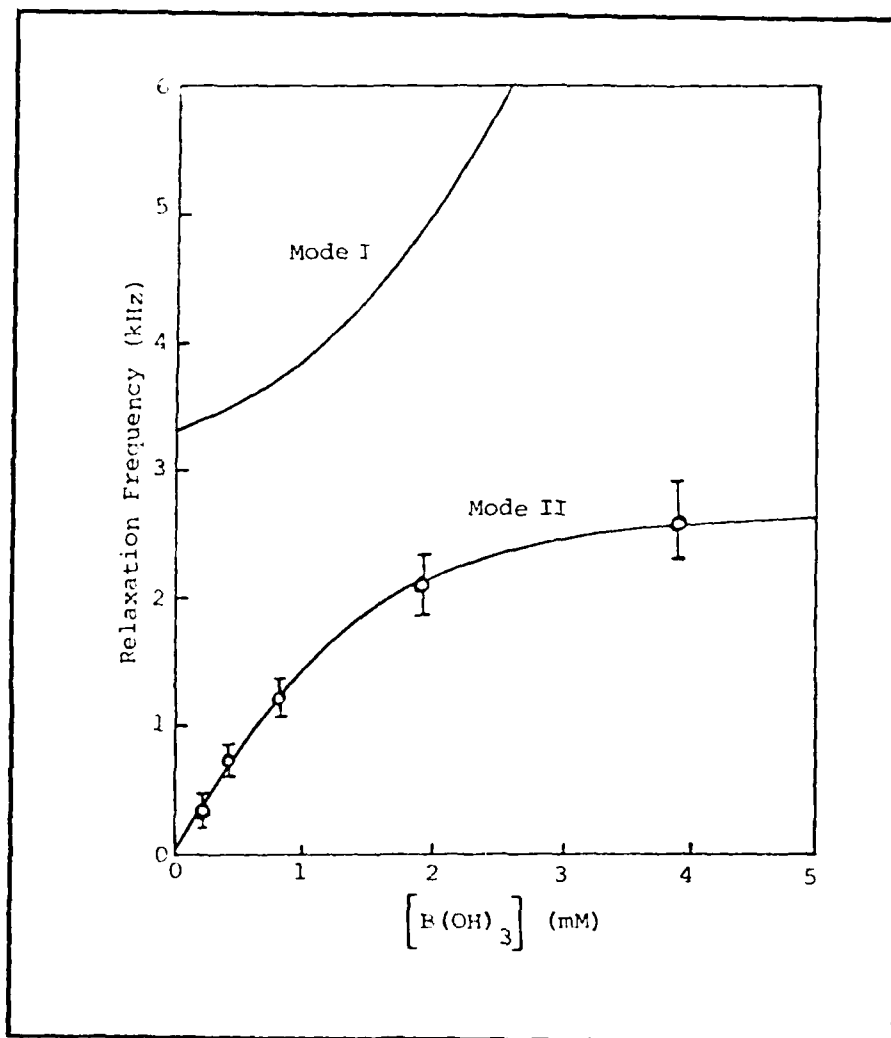


Figure 3-3. T-jump Measurements of  $B(OH)_3$  Relaxation Frequency in NaCl Solution Compared with Present Theory

are given in table 3-1. Note that, although the higher mode I falls in the experimental range, the effects may not be noticeable if the excitation is small.

Table 3-1.  $B(OH)_3$  Rate and Equilibrium Constants  
in NaCl Solution (Present Theory)

$$k_2^- = 7.5 \times 10^2 /s$$

$$k_2^+ = 1.7 \times 10^4 /s$$

$$K_2 = 23$$

$$k_1^+ = 1.2 \times 10^7 /M \cdot s$$

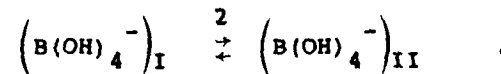
$$k_1^- = 3.3 \times 10^3 /s$$

$$K_1^* = 3.6 \times 10^3 /M$$

In the normal mode model for aqueous  $B(OH)_3$ , the two asymptotic equilibria are



and



However, the relaxation frequency  $\omega_1$  is not always greater than  $\omega_2$  as it would be in the diffusion-controlled case. For the coupled system, the two conditions are given by the following approximation:

$$\left. \begin{aligned} \omega_{II} &\approx \frac{k_1^-}{1+K_2} + k_1^+ \left[ B(OH)_3 \right] \\ \omega_I &\approx k_2^- + k_2^+ + \frac{k_1^- K_2}{1+K_2} \end{aligned} \right\} \omega_1 \ll \omega_2$$

(3-4)

$$\left. \begin{aligned} \omega_{II} &\approx k_2^- + \frac{k_2^+ K_1 \left[ B(OH)_3 \right]}{1 + K_1 \left[ B(OH)_3 \right]} \\ \omega_I &\approx k_1^- + k_1^+ \left[ B(OH)_3 \right] + k_2^- \end{aligned} \right\} \omega_1 \gg \omega_2$$

Simmons' measurements show no measureable changes with temperature which indicates that all temperature variation in the equilibrium constant comes from  $k_2^-$ . This conclusion is also supported by the rather large temperature dependence of  $\alpha_{max}$ . Excitation of step 1, via step 2 is, therefore, small for  $\omega_1 \gg \omega_2$  and the lower mode dominates pH change throughout.

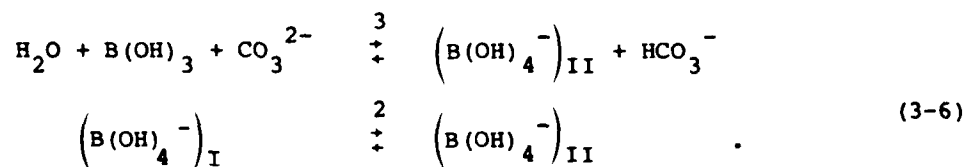
In the case of  $\alpha_{max}$ , the upper mode is directly excited through  $\Delta V_2$  at small concentrations. The resulting absorption is small and the relaxation frequency is still well below the range of present equipment. At higher concentration, the upper mode is not excited because  $\Delta V_1 = 0$  and the lower mode dominates.

In the SSW model, only step 4 is assumed to be diffusion-controlled. Then the rate equation (2-45) can be approximated to give the following determinant:

$$\begin{vmatrix}
 k_1^- + k_1^+ [B(OH)_3] + k_3^+ [CO_3^{2-}] - \omega_r & k_1^- - k_3^- [HCO_3^-] & (k_1^+ - k_3^+) [B(OH)_3] - k_3^- [B(OH)_4^-] \\
 k_2^+ - k_3^+ [CO_3^{2-}] & k_2^- + k_2^+ + k_3^- [HCO_3^-] - \omega_r & k_3^+ [B(OH)_3] + k_3^- [B(OH)_4^-] \\
 k_4^+ [HCO_3^-] & 0 & k_4^- + k_4^+ [HCO_3^-] - \omega_r
 \end{vmatrix}$$

(3-5)

For  $[CO_2] = 0$ , equation (3-5) reduces to equation (3-2). The third relaxation frequency is above the range of interest and can be neglected. The other two are shown in figure 3-4. In this case, it is convenient to consider the asymptotic equilibria



In the coupled system, including step 1, the conditions are given by the following approximations for  $\omega_3 \ll \omega_2$ ,

$$\begin{aligned}
 \omega_I &\approx k_2^- + k_2^+ + k_1^- \\
 \omega_{II} &\approx k_3^- \left( [HCO_3^-] + [B(OH)_4^-] \right) + k_3^+ \left( [B(OH)_3] + [CO_3^{2-}] \right)
 \end{aligned}$$

(3-7)

and for  $\omega_3 \gg \omega_2$ ,

$$\begin{aligned}
 \omega_I &\approx k_3^- \left( [HCO_3^-] + [B(OH)_4^-] \right) + k_3^+ \left( [B(OH)_3] + [CO_3^{2-}] \right) \\
 \omega_{II} &\approx k_2^- + k_2^+ + k_1^-
 \end{aligned}$$

(3-8)

Thus, there is a rapid and complete mode change. In this case, pH change follows the lower mode, while the absorption dominated by the exchange path branches to the upper mode. The short-circuit condition mentioned earlier is clearly governed by  $k_1^-$ . For the diffusion-controlled case,  $k_1^- \gg k_2^- + k_2^+$ , and the transition would be above the range of interest.

The present model does not resolve the pH discrepancy in figure 3-2, since the relaxation should follow the exchange. However, at pH = 9.5, sea water is highly supersaturated with  $\text{CaCO}_3$  and precipitation could account for the reduced value.

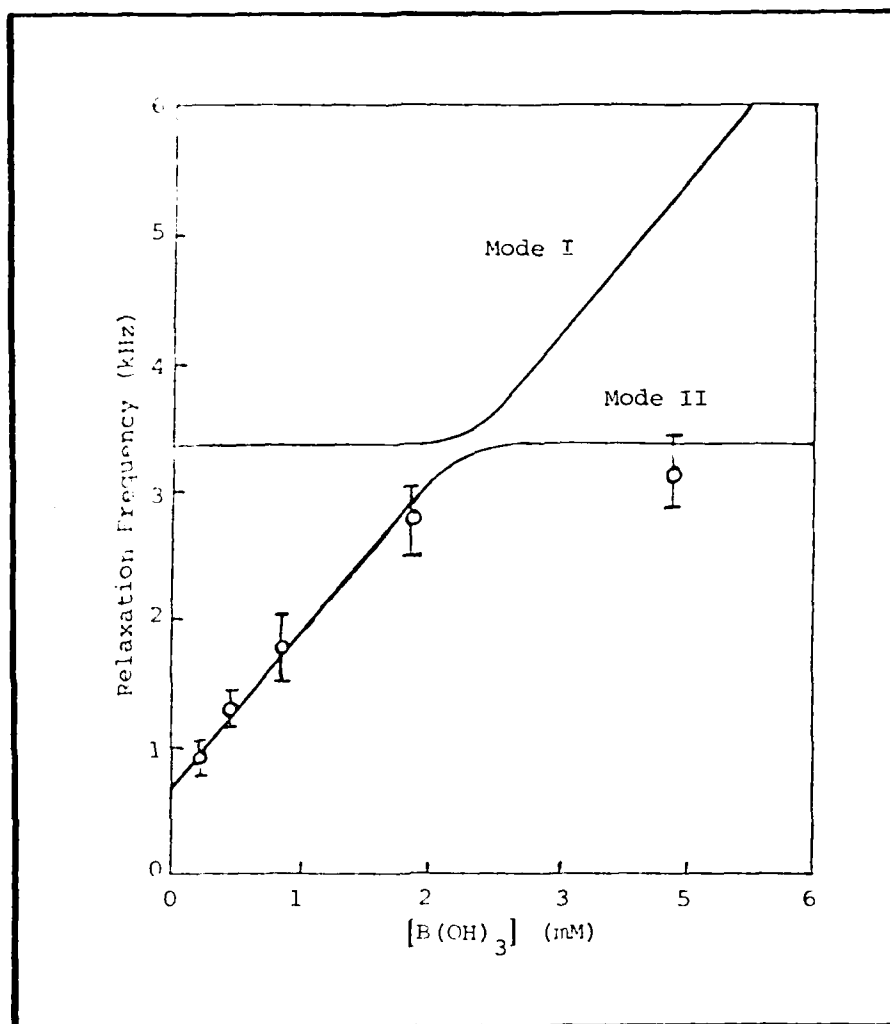


Figure 3-4. T-jump Measurements of  $B(OH)_3$  Relaxation Frequency in SSW Compared With Present Theory

## Section 4

## CONCLUSIONS

→ Resonator measurements indicate that the principal  $B(OH)_3$  absorption mechanism in sea water is an exchange between the  $B(OH)_3/B(OH)_4^-$  and  $HCO_3^-/CO_3^{2-}$  equilibria in which coupling to the  $Ca^{2+}$  ion-pairing equilibria provides most of the molal volume change. If either Ca or  $CO_2$  are omitted,  $B(OH)_3$  absorption is an order of magnitude too low.

T-jump measurements indicate a two-step  $B(OH)_3$  ionization process in  $H_2O$ . In sea water, both relaxations occur and are coupled. Present theory shows that pH and absorption may have different relaxation frequencies as experimental data indicates.

The empirical pH-dependent absorption formula derived from ocean measurements gives predictions that are consistent with the exchange relaxation model. ←

## REFERENCES

1. E. B. Stephenson, "Transmission of Sound in Sea Water: Absorption and Reflection Coefficients and Temperature Gradients," NRL Report No. S-1204, Naval Research Laboratory, Washington, D.C., 1935.
2. L. N. Liebermann, "Origin of Sound Absorption in Water and in Sea Water," Journal of the Acoustical Society of America, vol. 20, no. 6, pp. 868-873, 1948.
3. R. W. Leonard, P. C. Combs and L. R. Skidmore, "Attenuation of Sound in Synthetic Sea Water," Journal of the Acoustical Society of America, vol. 21, no. 1, p. 63, 1949.
4. O. B. Wilson and R. W. Leonard, "Measurements of Sound Absorption in Aqueous Salt Solutions by a Resonator Method," Journal of the Acoustical Society of America, vol. 26, no. 2, pp. 223-228, 1954.
5. G. Kurtze and K. Tamm, "Measurement of Sound Absorption in Water and in Aqueous Solutions of Electrolytes," Acustica, vol. 3, pp. 33-48, 1953.
6. M. Eigen and K. Tamm, "Sound Absorption in Electrolytic Solutions Due to Chemical Relaxation," Z. Electrochem, vol. 66, pp. 93-121, 1962. English translation Scripps Institute of Oceanography Document No. SIO, pp. 68-41, 1968.
7. M. Schulkin and H. W. Marsh, "Sound Absorption in Sea Water," Journal of the Acoustical Society of America, vol. 35, no. 5, pp. 864-865, 1962.
8. W. H. Thorp, "Deep-Ocean Sound Attenuation in the Sub- and Low-Kilocycle-Per-Second Range," Journal of the Acoustical Society of America, vol. 38, no. 4, pp. 648-654, 1965.

## REFERENCES (cont'd)

9. W. H. Thorp, "Analytic Description of the Low-Frequency Attenuation Coefficient," Journal of the Acoustical Society of America, vol. 42, no. 1, pp. 270-271, 1967.
10. A. Skretting and C. C. Leroy, "Sound Attenuation Between 200 Hz and 10 kHz," Journal of the Acoustical Society of America, vol. 49, no. 1, pp. 276-281, 1971.
11. D. G. Browning and W. H. Thorp, Attenuation of Low-Frequency Sound in the Ocean, NUSC Technical Report No. 4581, Naval Underwater Systems Center, New London, CT, 1972.
12. NUSC Scientific and Engineering Studies, "Attenuation of Low-Frequency Sound in the Sea," vol. I and II, Naval Underwater Systems Center, New London, CT, 1981.
13. D. G. Browning, E. N. Jones, R. H. Mellen and W. H. Thorp, "Attenuation of Low-Frequency Sound in Fresh Water," Science, vol. 162, pp. 1120-1121, 1968.
14. D. G. Browning, J. M. Gorman, E. N. Jones, W. H. Thorp and R. H. Mellen, "Lake Tanganyika Sound Attenuation Experiment," Nature Physical Science, vol. 240, pp. 86-87, 1972.
15. R. H. Mellen and D. G. Browning, "Attenuation in Randomly Inhomogeneous Sound Channels," Journal of the Acoustical Society of America, vol. 56, no. 1, pp. 80-82, 1974.
16. R. H. Mellen, D. G. Browning and V. P. Simmons, "Acoustic Attenuation in Lake Tanganyika," Nature, vol. 277, pp. 374-375, 1979.

## REFERENCES (cont'd)

17. R. H. Mellen, D. G. Browning and V. P. Simmons, "Acoustic Absorption by  $\text{MgCO}_3^{\circ}$  Ion-Pair Relaxation," Nature, vol. 279, pp. 705-706, 1979.
18. R. H. Mellen and D. G. Browning, "Variability of Low-Frequency Sound Absorption in the Ocean: pH Dependence," Journal of the Acoustical Society of America, vol. 61, no. 3, pp. 704-706, 1977.
19. E. Yeager, F. H. Fisher, J. Miceli and R. Bressel, "Origin of Low-Frequency Sound Absorption in Sea Water," Journal of the Acoustical Society of America, vol. 53, no. 6, pp. 1705-1707, 1973.
20. V. P. Simmons, "Investigation of the 1-kHz Sound Absorption in Sea Water," Ph.D. Thesis, Department of Oceanography, University of California, San Diego, CA, 1975.
21. R. H. Mellen, V. P. Simmons and D. G. Browning, "Sound Absorption in Sea Water: A Third Chemical Relaxation," Journal of the Acoustical Society of America, vol. 65, no. 4, pp. 923-925, 1979.
22. R. H. Mellen, V. P. Simmons and D. G. Browning, "Low-frequency Sound Absorption in Sea Water: A Borate-Complex Relaxation," Journal of the Acoustical Society of America, vol. 67, no. 1, pp. 341-342, 1980.
23. R. H. Mellen, D. G. Browning and V. P. Simmons, "Investigation of Chemical Sound Absorption in Sea Water by the Resonator Method: Part I," Journal of the Acoustical Society of America, vol. 68, no. 1, pp. 248-257, 1980; Part II, Journal of the Acoustical Society of America, vol. 69, no. 6, pp. 1660-1662, 1981; Part III, Journal of the Acoustical Society of America, vol. 70, no. 1, pp. 143-148, 1981.

## REFERENCES (cont'd)

24. A. Disteche, "The Effect of Pressure on Dissociation Constants and Its Temperature Dependency," The Sea, edited by A. Goldberg, Wiley Interscience, New York, 1974, vol. 5, ch. 2, pp. 81-121.
25. J. Lyman, "Buffer Mechanism in Sea Water," Ph.D. Thesis, University of California, Los Angeles, CA, 1957.
26. G. K. Ward and F. J. Millero, "The Effect of Pressure on the Ionization of Boric Acid in Aqueous Solutions From Molal Volume Data," Journal of Solution Chemistry, vol. 3, pp. 417-430, 1974.
27. J. Stuehr and E. Yeager, "The Propagation of Ultrasonic Waves in Electrolytic Solutions," Physical Acoustics, edited by W. P. Mason, Academic, New York, 1965, vol. II, part A, ch. 6, pp. 376-452.
28. M. Eigen, "Proton Transfer, Acid-Base Catalysis and Enzymatic Hydrolysis, Part I: Elementary Processes," Angewandte Chemie (International Edition), vol. 3, pp. 1-172, 1964.
29. R. P. Bell, J. O. Edwards and R. B. Jones, "The Structure and Acidity of Boric Acid and Their Relation to Reaction Mechanisms," The Chemistry of Boron and Its Compounds, edited by E. L. Muetterties, Wiley, New York, 1963, ch. 4, pp. 209-221.
30. M. Schulkin and H. W. Marsh, "Low-Frequency Sound Absorption in the Ocean," Journal of the Acoustical Society of America, vol. 63, no. 1, pp. 43-48, 1978.
31. J. R. Lovett, "Geographical Variation of Low-Frequency Sound Absorption in the Atlantic, Indian and Pacific Oceans," Journal of the Acoustical Society of America, vol. 67, no. 1, pp. 338-340, 1980.

**DATA  
FILM**